Can Cloud Seeding Help Tackle Delhi's Air Pollution?

A

Report

Centre for Atmospheric Sciences (CAS)

Indian Institute of Technology Delhi

New Delhi - 110016

October 2025

Prepared by (In alphabetical Order):

Aasif Ahmad Wagay, Aiswarya Ramachandran, Alice Jeeva P J, Anirudh K M, Aparna Aparajita, Ardra D, Chaithra S T, Charudatt J Puri, Debjit Paul, Dhishana P R, Emili Singha Roy, Gobinda Manna, Joswin P Joy, Pankaj Lal Sahu, Payel Kundu, Rupanjan Banerjee, Sanya Narbar, Saran Rajendran, Shreya Srivastava, Sojol Das, Subhadeep Ghosh, Tanerao Singh Sankhla, and Vasu Singh

Mentors (In alphabetical Order):

Prof. Krishna Mirle Achutarao, Prof. Sagnik Dey, Prof. Sajeev Philip, Prof. Sandeep Sukumaran, and Prof. Shahzad Gani

Executive Summary

This report assesses the atmospheric feasibility of utilizing cloud seeding as a strategy to mitigate severe winter air pollution in Delhi. A comprehensive analysis, integrating climatological data (2011-2021), aerosol-cloud interaction assessments, and pollutant washout/recovery, leads to the primary conclusion that Delhi's winter atmosphere is climatologically unsuitable for consistent and effective cloud seeding.

There is a fundamental lack of sufficient moisture and saturation during the peak pollution months (December-January), coinciding precisely when intervention is most needed. While Western Disturbances (WDs) are the primary drivers of potential seeding conditions, viable "windows of opportunity" are rare, confined to specific anomalous events. Even on days identified as potentially promising (e.g., cloudy WD days without rain), a multi-criteria Moisture Suitability Index (MSI) indicates they frequently lack the necessary combination of moisture depth, saturation, and atmospheric lift required for successful seeding.

Furthermore, the study highlights complexities arising from Delhi's high aerosol environment. High aerosol loading (characterized by high Aerosol Optical Depth; AOD) is associated with increased cloud cover and higher liquid/ice water content, particularly during rainy conditions. However, favorable microphysical conditions (low cloud base, high water content) often coincide with naturally occurring precipitation, limiting the potential added benefit of seeding. The vertical separation between the shallow aerosol layer (below 2 km) and typical seedable cloud layers (2-5 km) also presents significant operational targeting challenges. Thermally, glaciogenic seeding appears potentially viable during core winter, but operational feasibility seems restricted to existing rainy conditions.

Regarding pollution removal, the analysis confirms that heavy natural rainfall is highly effective (>80-95% washout for $PM_{2.5}$, PM_{10}, NO_X), while light rain offers minimal impact. Importantly, even after significant washout, air quality improvements are short-lived, with pollutant concentrations typically recovering to pre-event levels within 1-5 days due to persistent emissions. Ozone concentrations often increase post-rainfall. While dry WDs provide some limited ventilation, significant concerns remain regarding the environmental/health impacts of seeding agents like AgI, high operational costs, and scientific uncertainties.

Given these constraints, cloud seeding cannot be recommended as a primary or reliable strategy for Delhi's winter air pollution management. It should be viewed, at best, as a potential high-cost,

emergency short-term measure, contingent on stringent forecasting criteria. The study underscores that sustained emission reduction remains the most viable and necessary long-term solution.

Disclosure: This study and report were produced during a Hackathon on the topic held between 13-15 October 2025 at the Centre for Atmospheric Sciences (CAS) IIT Delhi. The participants were PhD students at CAS who received mentorship from CAS faculty. This study has not been through any peer review at this time. Artificial intelligence (AI) language models were utilized during the preparation of this report.

Contact for Further Details:

Head,
Centre for Atmospheric Sciences
Indian Institute of Technology Delhi
Hauz Khas, New Delhi 110016
Email: hodcas@admin.iitd.ac.in

Background

The National Capital Region (NCR) of India, centred around Delhi, faces an escalating air quality crisis, particularly during the winter months (October-February). High emission rates from diverse sources - including vehicular traffic, industrial activities, construction dust, agricultural biomass burning, and residential heating - combine with unfavorable meteorological conditions to create prolonged episodes of severe pollution. Winter meteorology is characterized by low temperatures, weak winds, frequent thermal inversions, and a shallow planetary boundary layer (PBL), which collectively trap pollutants near the surface, leading to hazardous concentrations of particulate matter (PM2.5, PM10) and other harmful substances often exceeding international health guidelines manifold.

Historically, the primary natural mechanism for cleansing Delhi's atmosphere during winter has been precipitation associated with the passage of Western Disturbances (WDs). These synoptic-scale weather systems, originating in the Mediterranean region, travel eastward and bring moisture into Northwest India. Sufficiently strong WDs can induce widespread light-to-moderate rainfall, which effectively scavenges airborne pollutants through processes like nucleation scavenging within clouds and impaction scavenging below clouds. Studies have shown significant improvements in air quality following such rain events.

However, the frequency and intensity of rain-bearing WDs are variable, and recent climate projections suggest a potential decline in their occurrence, raising concerns about the future reliability of this natural cleansing process. Furthermore, many WDs are weak or dry, bringing cloud cover and humidity but failing to produce substantial rainfall, sometimes even exacerbating pollution by strengthening temperature inversions. The inability of the atmosphere to naturally cleanse itself frequently during peak pollution periods underscores the need to explore alternative mitigation strategies.

Cloud seeding emerges as one such potential intervention. It is a form of weather modification that aims to enhance precipitation from existing clouds by introducing artificial aerosol particles that can act as efficient Cloud Condensation Nuclei (CCN) or Ice Nucleating Particles (INP). Common methods include hygroscopic seeding (using salts like NaCl or $CaCl_2$ in warm clouds to accelerate droplet coalescence) and glaciogenic seeding (using agents like silver iodide (AgI) or dry ice in cold clouds containing supercooled water to promote ice crystal formation). While primarily developed and operationally used for augmenting water supplies in arid and semi-arid

regions, including extensive programs in India, the potential application of cloud seeding for air pollution reduction via enhanced wet deposition is a relatively new but increasingly relevant area of investigation. The severe air quality situation in Delhi, coupled with the known effectiveness of natural rain in clearing pollutants, makes it an important test case for assessing the feasibility of this approach. This report evaluates the atmospheric conditions necessary for successful cloud seeding during Delhi's winter, examines the influence of the region's high aerosol loading on cloud properties, and analyses the efficiency and longevity of pollutant removal by precipitation, providing an assessment of whether cloud seeding can be a viable tool in tackling the city's air pollution crisis.

List of Abbreviations

AgI: Silver Iodide

AOD: Aerosol Optical Depth

CAAQMS: Continuous Ambient Air Quality Monitoring Stations

CAPE: Convective Available Potential Energy

CBH: Cloud Base Height

CC: Cloud Cover

CCN: Cloud Condensation Nuclei

CDNC: Cloud Droplet Number Concentration

CPCB: Central Pollution Control Board

GCCN: Giant Cloud Condensation Nuclei

IN: Ice Nuclei

INP: Ice Nucleating Particles

LWC: Liquid Water Content

MSI: Moisture Suitability Index

NCR: National Capital Region

NOX: Nitrogen Oxides (NO & NO_2)

NWDNR: Non-Western Disturbance Non-Rainy Days

NWDR: Non-Western Disturbance Rainy Days

PBL: Planetary Boundary Layer

PM2.5: Particulate Matter with aerodynamic diameter ≤ 2.5 μm

PM10: Particulate Matter with aerodynamic diameter ≤ 10 μm

RH: Relative Humidity

SNA: Sulfate, Nitrate, Ammonium

TCWV: Total Column Water Vapour

WD: Western Disturbances

WDNR: Western Disturbance Non-Rainy Days

WDR: Western Disturbance Rainy Days

Table of Contents

1. Assessment of Atmospheric Moisture, Dynamics and Thermodynamics

1.1 Introduction

Water scarcity and severe air pollution are among the most critical environmental challenges facing urban centres worldwide, particularly in megacities such as New Delhi. Natural precipitation plays an important role in both problems; it replenishes water resources and effectively removes pollutants from the atmosphere through washout. Given the significance of rainfall, weather modification through cloud seeding has long been explored as a potential tool for augmenting water supplies, especially in drought-prone regions. The primary methods of cloud seeding (static, dynamic, and hygroscopic) have a long history of application in India for drought mitigation (Malik et al., 2018). These techniques aim to enhance a cloud's natural precipitation efficiency by introducing specific aerosol particles, such as silver iodide or hygroscopic salts, to alter its microphysical processes (Malik et al., 2018).

Despite its long history and continued use in operational programs worldwide, cloud seeding remains a scientifically contentious field. As highlighted in a foundational review by Bruintjes (1999), definitively proving the effectiveness of any seeding operation is inherently difficult. The immense natural variability of cloud systems makes it challenging to distinguish a modest, human-induced effect from what would have occurred naturally, a problem often referred to as the "black box" of weather modification (Bruintjes, 1999). This persistent uncertainty has led to a divide between the operational needs of water managers and the rigorous level of proof required by the scientific community. Malik et al. (2018) present a balanced perspective, framing cloud seeding as a potentially valuable tool for water resource management while also emphasising its environmental implications, high operational costs, and the continuing lack of conclusive scientific evidence for its effectiveness.

In Delhi, the context is further complicated by unique winter meteorological conditions and a severe, recurring air pollution crisis. Winter (late October-February) is characterised by low temperatures (falling to 3°C in January) for Delhi, scarce rainfall primarily dominated by WDs, and northwesterly winds. This winter rainfall constitutes around 15% of the yearly precipitation over northwest India, crucial for the rabi crop (Yadav et al., 2012). Delhi's winter rainfall is relatively scarce and primarily associated with WDs traversing the Himalayas, bringing occasional light to moderate precipitation (Hunt et al., 2025). Critically, a shallow planetary boundary layer

(PBL) often forms due to severe thermal inversions, trapping pollutants and leading to severe air pollution episodes (Arun et al., 2018; Murthy et al., 2020). Thermodynamic conditions exhibit weak instability due to these inversions, with low Convective Available Potential Energy (CAPE) values compared to summer, highlighting WDs as the primary synoptic driver for winter precipitation (Kumar et al., 2024).

For decades, strong WDs bringing widespread rain have been the city's primary natural cleansing mechanism, effectively scavenging pollutants like PM2.5 (Particulate Matter with aerodynamic diameter $\leq$ 2.5 μm) and PM10 (Particulate Matter with aerodynamic diameter $\leq$ 10 μm) and improving air quality (Hunt et al., 2025; Xie et al., 2024). The efficiency of this washout increases with rainfall intensity and duration (Chowdhury et al., 2016; Luan et al., 2019; Roy et al., 2019). However, recent climate projections show a robust declining trend in WD frequency, suggesting this natural cleansing mechanism is becoming less reliable (Hunt et al., 2019). Furthermore, many WDs are "weak" or "dry", increasing cloud cover and humidity but failing to produce sufficient rain, sometimes worsening pollution by strengthening inversions.

This confluence of severe air pollution and the declining reliability of natural cleansing mechanisms has intensified interest in exploring artificial solutions like cloud seeding in Delhi. The growing understanding of how anthropogenic air pollution itself impacts clouds adds another dimension. Research by Givati and Rosenfeld (2005) established that air pollution (by adding numerous small CCN) can suppress natural precipitation, paradoxically suggesting that these same polluted clouds might be more susceptible to enhancement through seeding, which aims to counteract this suppression effect. This has opened a new frontier for cloud seeding research: its direct application as an air quality improvement tool. Theoretical models (Agrawal et al., 2024) and preliminary field experiments (Ku et al., 2023) suggest seeding can enhance rainfall to mitigate pollutant concentrations. Pilot projects, such as one initiated by IIT Kanpur, are exploring this potential for Delhi's winter. While concerns about cost and the environmental impact of seeding agents like silver iodide remain (Fajardo et al., 2016), the scale of Delhi's public health crisis necessitates investigating cloud seeding as a potential emergency response tool, rather than a permanent solution.

However, the success of any seeding operation is fundamentally constrained by pre-existing atmospheric conditions. For seeding to be viable, a "window of opportunity" must exist, characterised by sufficient atmospheric moisture, favourable cloud dynamics (including cloud condensation nuclei characteristics), and an environment conducive to precipitation growth.

Critical knowledge gaps remain in systematically assessing these conditions, identifying days with moisture and cloud cover comparable to naturally rainy days (>7.5mm), and understanding pollutant recovery dynamics post-rainfall, especially during Delhi's severe pollution episodes. This chapter analyses the winter climatology of key atmospheric variables over Delhi and develops the MSI to quantify the frequency of conducive conditions and identifies days with moisture content and cloud cover comparable to those experiencing natural moderate to heavy rainfall (>7.5mm).

1.2 Data and Methods

1.2.1 Study Region

The analysis focuses on two nested geographical domains (Figure 1):

- An inner domain centred directly over Delhi (28.4°-29°N, 76.8°-77.4°E), used for detailed local analysis.
- A broader outer domain covering the larger North Indian plains (27°-32°N, 74°-81°E), used to analyse the synoptic-scale weather patterns that influence the region, such as Western Disturbances.

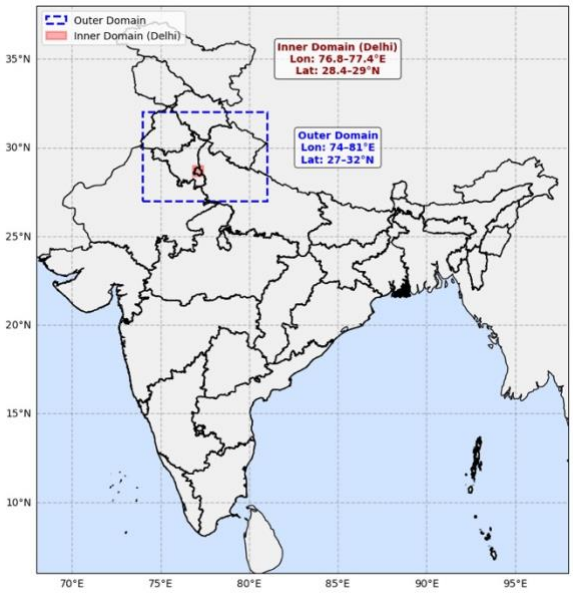

Figure 1:Study area.

We considered a domain that covers the entire Delhi-NCR region for the study. We selected only those WDs that could potentially influence the NCR region by considering NCR as the centre and applying a 1000 km buffer around it, corresponding to the characteristic spatial scale of a WD, which typically has a diameter of about 1000 km (Hunt et al., 2018).

1.2.2 Data and Variables

The primary data source for this research is the ERA5 global atmospheric reanalysis dataset, produced by the European Centre for Medium-Range Weather Forecasts (ECMWF). We utilise hourly data with a spatial resolution of 0.25° x 0.25° for the winter months (October through February) spanning a decadal period from 2011 to 2021.

We use the following atmospheric variables for the analysis.

- Total Column Water Vapour (TCWV): Represents the total integrated amount of water vapour in a vertical column of the atmosphere (mm), providing a measure of the depth and overall size of the moisture reservoir.
- Temperature (t): Used to determine the thermal properties of the atmospheric layer, which is critical for identifying whether conditions are suitable for warm-cloud (hygroscopic) or cold-cloud (glaciogenic) seeding.
- Relative Humidity (r): This percentage value indicates the air's proximity to saturation, a direct requirement for cloud droplet formation and persistence.
- Specific Cloud Liquid Water Content (CLWC): This measures the mass of liquid water droplets (g/kg) already present in the cloud. A non-zero value is critical as it represents the actual “seedable medium” that seeding agents would interact with.
- Vertical Velocity (omega): This variable measures large-scale atmospheric motion (Pa/s). A negative value indicates rising air (lift), which drives cloud development and is essential for a successful seeding operation.

Humidity data used to calculate column integrated humidity was obtained from the ERA5 global reanalysis with resolution 0.25° x 0.25° (Hersbach et al., 2020).

1.2.3 Methods

Climatological Baseline

A long-term climatology was first established for each variable by calculating the monthly mean for all winter months over the 2011-2021 period. This baseline represents the "normal" atmospheric state for Delhi's winters and serves as a reference against which specific weather events can be compared.

The Moisture Suitability Index (MSI)

The MSI is a 5-point scoring system applied to daily-averaged data. For each day in the study period, a score is calculated by awarding one point for each of the following six criteria that are met:

1. Presence of Cloud for Seeding: Cloud Fraction >= 0.25.
2. Saturation check: Relative Humidity (RH) averaged between 850 hPa and 600 hPa > 60%.
3. Fuel check: Liquid Water Content (LWC, at 850 hPa) > 0.5 g m^{-3} .
4. Level of freezing: 0°C line should be at 700 hPa or above.
5. Lift Check: Vertical velocity (w) at 850 hPa > 1.5 m s^{-1}.

Days are then categorised based on their final score. The final output is a quantitative summary detailing the frequency of suitable days, providing a robust, multi-faceted assessment of cloud seeding potential.

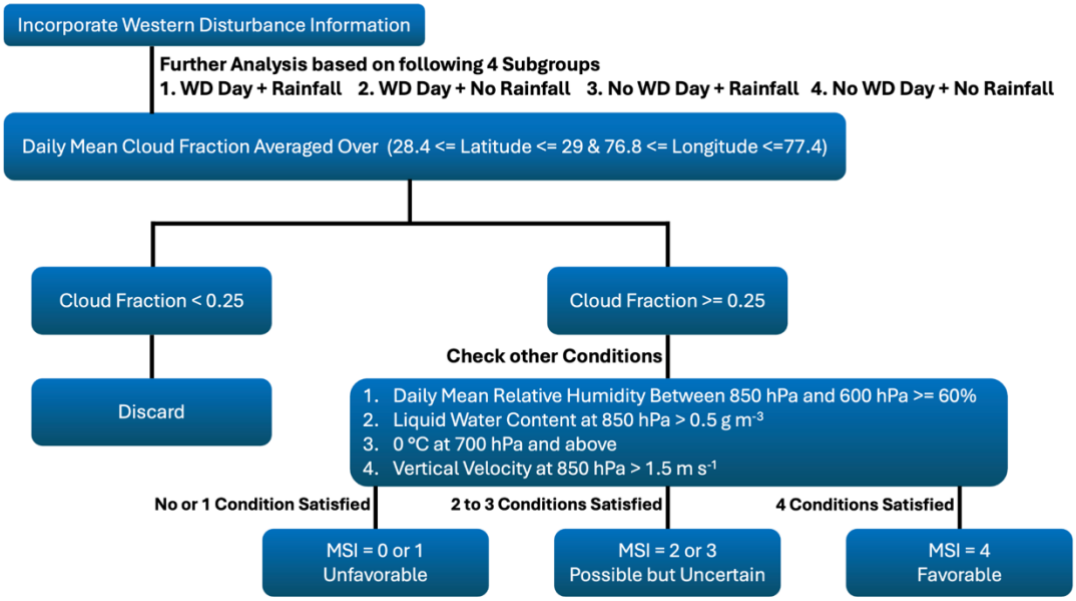

Figure 2: Flowchart for the calculation of MSI. The flowchart also shows the meteorological parameters considered and their corresponding thresholds.

Classification of Western Disturbances and Rainfall Intensity

The WDs whose tracks passed through this box between the months of October to February for the years 2011-2021 were selected. The WD tracks were obtained from Hunt et al. (2018). The identified WDs were then classified into rain-inducing and dry WDs.

The rainy days during the study period were classified as either WD-associated or locally induced, using the India Meteorological Department (IMD) daily gridded (0.25°x0.25°) rainfall data (Pai et al., 2014). The rainy days were further classified into light rainy days, which received rainfall less than 7.5mm and moderate to heavy rainy days (received more than 7.5mm rainfall) based on the rainfall intensity classification by IMD (https://imdpune.gov.in/Reports/glossary.pdf). The light rainy days were considered further to account for the possibility of rainfall enhancement by cloud seeding, and to find the days that are suitable for cloud seeding. The non-rainy days within the study period were filtered to find the days with moisture greater than the lower quartile of the moisture distribution of the rainy days.

The non-rainy days and light rain days with conditions conducive for cloud seeding were selected by defining thresholds for column-integrated specific humidity (q_int) from 100hPa to 300hPa and total cloud cover (CC). Days whose values of q_int and CC exceeded these thresholds were identified. The threshold for q_int and CC were defined as the values that divide the rainfall days into the 25th percentile (Figure 13, 14 and 15).

1.3 Results

1.3.1 Climatological Characteristics of Winter Months (Oct-Feb) Atmospheric Conditions over Delhi

Total Column Water Vapour

Figure 3 provides the climatological baseline for Total Column Water Vapour (TCWV) during Delhi's winter, revealing crucial patterns for assessing cloud seeding feasibility. A prominent seasonal drying trend is evident: October, retaining post-monsoon moisture, is the wettest month with TCWV often exceeding 15-18 mm. Moisture progressively decreases through November and December, with average values over Delhi dropping to 9-12 mm. January marks the climatological minimum, where TCWV across most of the region, including Delhi, falls below 9 mm, frequently

into the 3-6 mm range. A slight moisture increase occurs in February, likely associated with early Western Disturbances.

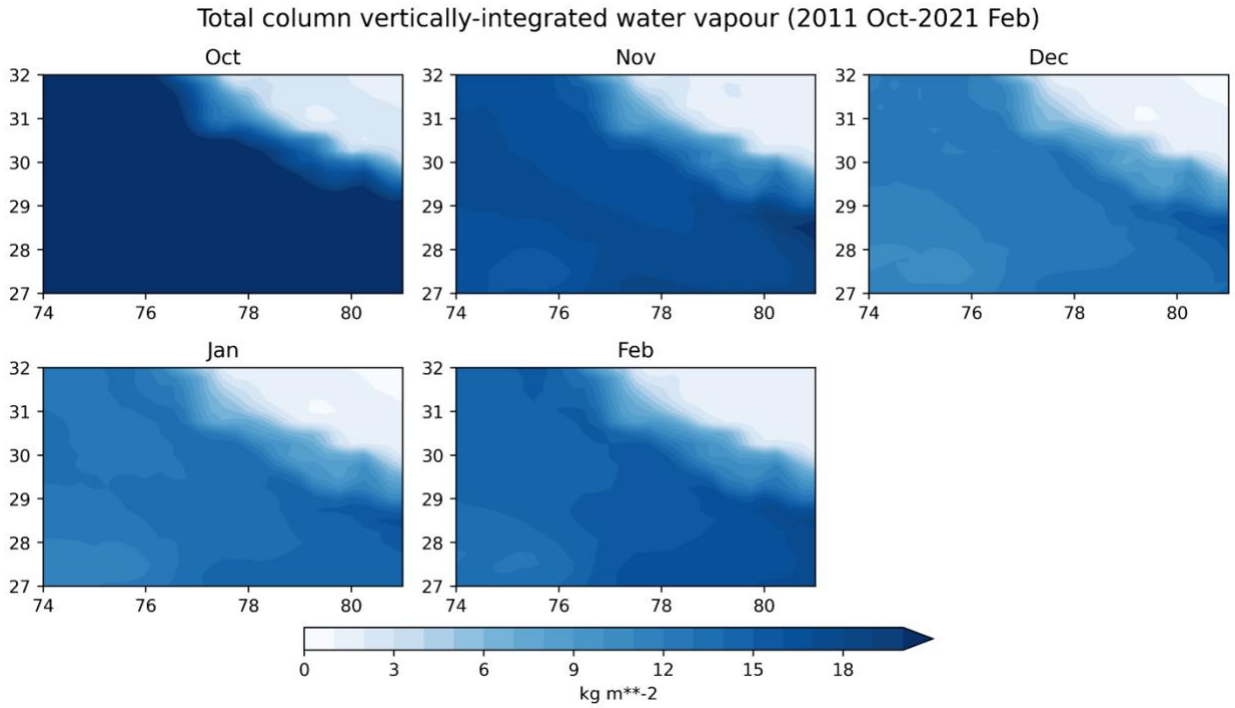

Figure 3: Monthly Climatology of TCWV over North India for winter months (October-February) from 2011 to 2021.

Alongside this seasonal change, a consistent spatial moisture gradient exists, oriented from the drier northwest (towards Punjab/Rajasthan) to the wetter southeast (towards Uttar Pradesh/Himalayan foothills, influenced by Bay of Bengal moisture and orographic effects). Delhi's location within this gradient subjects it to variable moisture depending on synoptic flow. Crucially, this analysis highlights that the period experiencing the most severe air pollution (December and January) coincides precisely with the driest atmospheric conditions. The average TCWV during these months falls significantly below typical thresholds considered necessary for successful cloud seeding, strongly suggesting that favourable conditions are not the norm. Therefore, viable opportunities for precipitation enhancement would likely be restricted to anomalous weather events, primarily strong Western Disturbances, capable of temporarily injecting sufficient moisture into the region to overcome the prevailing dry winter baseline.

Figure 4 shows the average diurnal cycle of TCWV over the study region, characterized by a consistent pattern across winter months. Driven by solar radiation, moisture levels typically reach a minimum in the early morning and peak in the early afternoon before declining. This analysis strongly reinforces the seasonal drying trend, with October being the moistest and

December/January the driest, showing clear separation in absolute TCWV values even between the daily maximums and minimums of different months. Notably, the inner domain (Delhi) is consistently moister than the broader outer domain, potentially due to local factors. While the diurnal peak in the early afternoon represents the most likely time for potential seeding, a significant challenge remains: even at this daily maximum, the absolute TCWV during the core winter months (December/January, ~10-13 mm) consistently falls below conservative thresholds for effective cloud seeding. This reinforces the conclusion that suitable conditions are likely anomalous rather than typical for Delhi's winter.

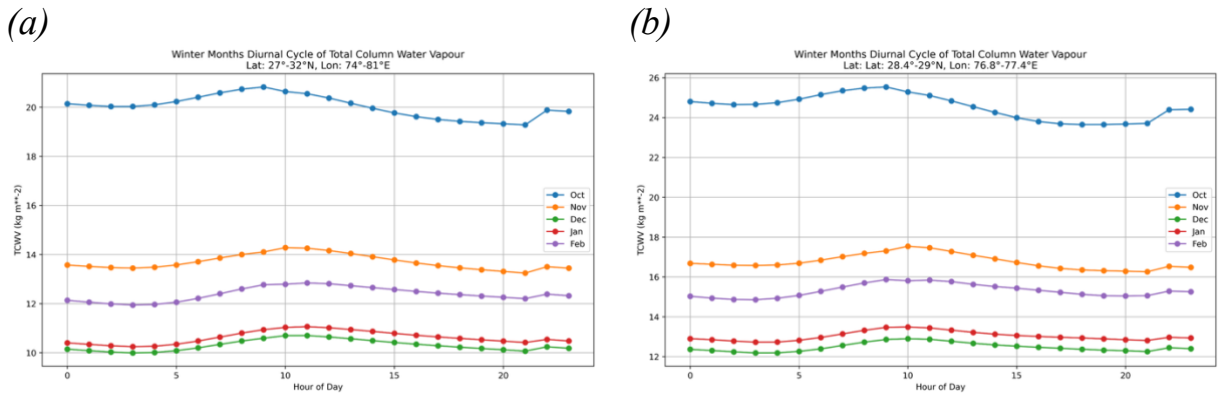

Figure 4: Mean diurnal cycle of TCWV for winter months (2011-2021) over (a) the inner Delhi domain (top panel) and (b) the broader outer domain (bottom panel). The plots show the spatially averaged TCWV (in kg m^{-2}) for each hour of the day (in UTC), illustrating the daily moisture pattern for each month.

Temperature

Figures 5 and 6 reveal the winter thermal structure over the study region, highlighting expected seasonal cooling (warmest in October, coldest in January) and a standard vertical temperature lapse rate, alongside a cooler northeastern spatial gradient. This thermal analysis is crucial for determining feasible cloud seeding strategies. The 850 hPa temperature shows a distinct seasonal transition: in October and November, it is consistently above freezing (0°C), defining a "warm cloud" environment suitable only for hygroscopic seeding. However, during the core winter months of December and January, the average 850 hPa temperature drops at or below freezing, creating the potential for supercooled liquid water. This shift makes glaciogenic (cold cloud) seeding theoretically possible during deep winter, contingent on the presence of sufficient cloud liquid water.

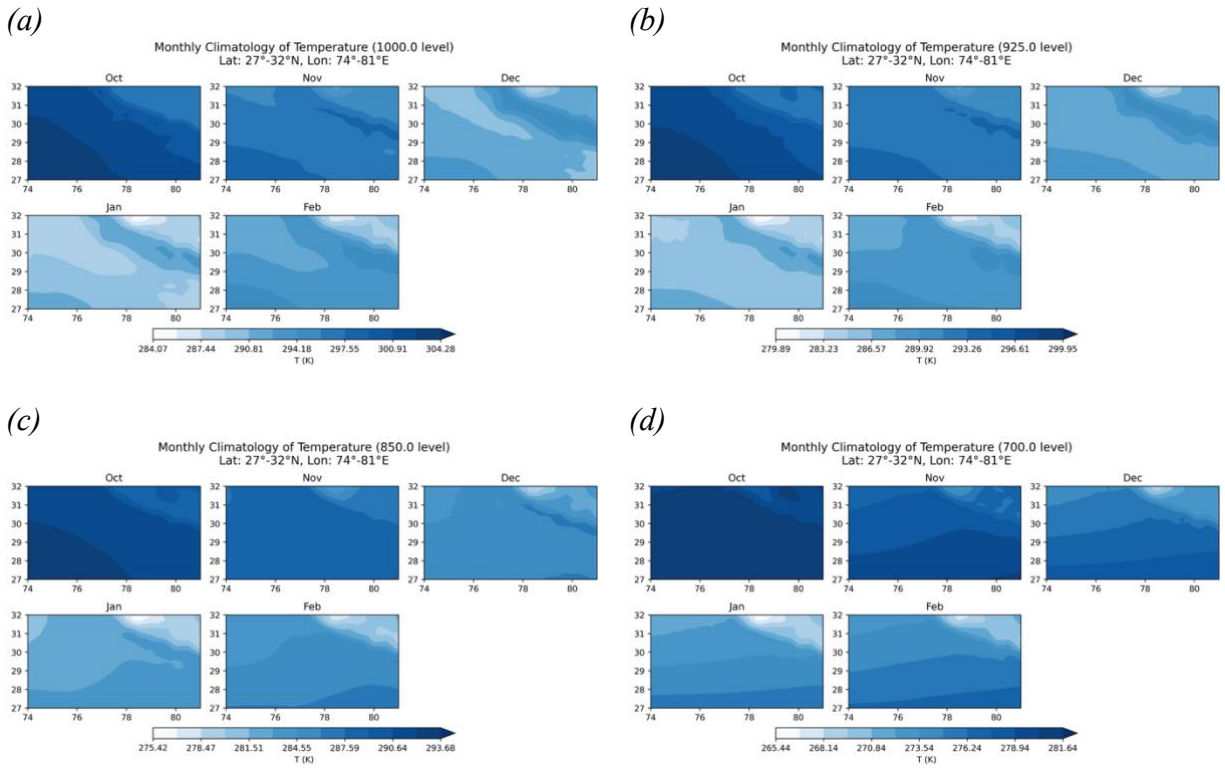

Figure 5: Monthly Climatology of temperature over North India for winter months (October-February) from 2011 to 2021. The panels show the long-term average spatial distribution of temperature (in Kelvin) at four different pressure levels: (a) 1000 hPa, (b) 925 hPa, (c) 850 hPa, and (d) 700 hPa.

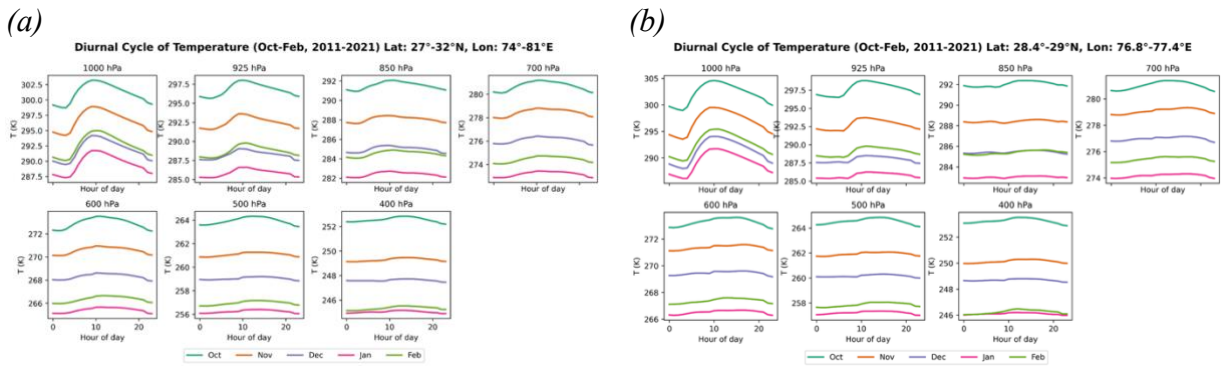

Figure 6: Mean diurnal cycle of Temperature (T) for the winter months (October-February) from 2011 to 2021. The panels show the average daily temperature pattern (in Kelvin) at various pressure levels for (a) the broader outer domain and (b) the inner Delhi domain. Each subplot corresponds to a specific pressure level, with colored lines representing the spatially averaged temperature for each hour of the day (UTC).

The diurnal temperature cycle (Figure 6), driven by solar heating, is a strong surface-level phenomenon with a 5-6 K range but weakens rapidly with altitude, becoming negligible at key cloud-forming levels like 850 hPa and above. At these altitudes, temperatures remain nearly constant throughout the day, primarily governed by the larger seasonal trend. This indicates that while moisture might peak in the afternoon, the critical thermal conditions dictating the

appropriate seeding methodology (hygroscopic vs. glaciogenic) are stable throughout the day and depend mainly on the specific winter month.

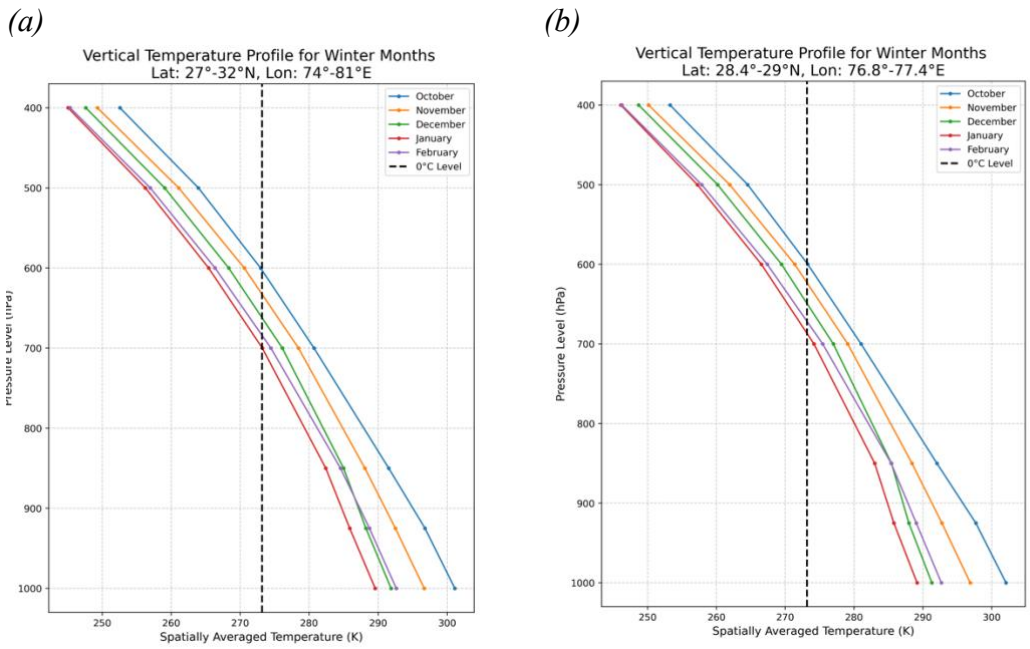

Figure 7: Vertical profiles of spatially averaged Temperature (T) for winter months (2011-2021). The plots show the change in mean temperature (K) with pressure level (hPa) for (a) the inner Delhi domain and (b) the broader outer domain. The dashed vertical line indicates the 0°C (273.15 K) freezing level.

The vertical temperature profiles (Figure 7) illustrate the atmosphere's thermal structure, showing a standard lapse rate and systematic cooling from October to a minimum in January. This seasonal evolution critically affects the height of the freezing level, which directly dictates the appropriate cloud seeding methodology. In early winter (Oct-Nov), the high freezing level ensures the 850 hPa layer is well above 0°C, classifying clouds as “warm” and making only hygroscopic seeding viable. Conversely, during core winter (Dec-Jan), the freezing level descends below 800 hPa, meaning the atmosphere at 850 hPa and above is, on average, below freezing; this creates the necessary thermal condition for supercooled liquid water, making glaciogenic (cold cloud) seeding theoretically possible, provided sufficient supercooled water exists.

Relative Humidity

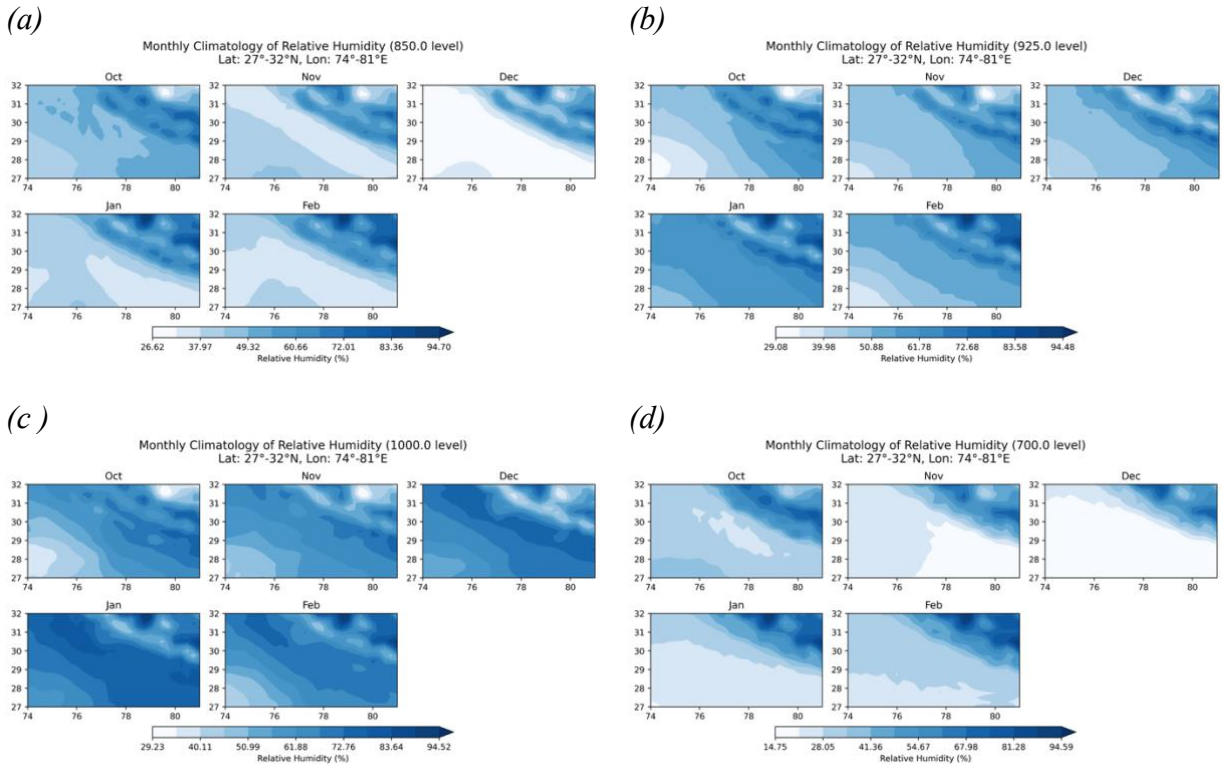

Figure 8: Monthly Climatology of Relative Humidity over North India for winter months (October-February) from 2011 to 2021. The panels show the long-term average spatial distribution of relative humidity (in %) at four different pressure levels: (a) 1000 hPa, (b) 925 hPa, (c) 850 hPa, and (d) 700 hPa.

The climatology of relative humidity (Figure 8) shows that the atmosphere over the region is, on average, far from saturation during the peak winter months. Spatially, the highest relative humidity is consistently found along the northeastern part of the domain, near the Himalayan foothills, where orographic lift forces air to cool and approach saturation. Seasonally, there is a significant drying trend from a relatively moist October to a much drier November and December, followed by a slight increase in January and February. The analysis of the 850 hPa level, which is critical for the MSI's "Saturation Check", is particularly showing. During the core winter months of December and January, the average relative humidity over most of the domain, including the Delhi region, is climatologically in the 50-70% range. This is well below the 80% threshold required for a successful Saturation Check, indicating that on a typical winter day, the air is too dry to support the formation and persistence of seedable clouds.

The diurnal variation of relative humidity (Figure 9) is a distinct boundary-layer feature that varies inversely with the daily temperature cycle. At the surface (1000 hPa), relative humidity is at its

maximum during the cool early morning hours and drops to a minimum during the warm afternoon. This strong daily swing weakens significantly with altitude, becoming much less defined by the 850 hPa level. Importantly, at this cloud-forming altitude, the average relative humidity during the core winter months of December and January consistently remains low, ranging between 40-60% in the outer domain and only slightly higher in the inner domain. These values are well below the 80% threshold required by the MSI's "Saturation Check," reinforcing the conclusion that the atmosphere is, on average, too dry to support cloud formation, even during its most humid part of the day.

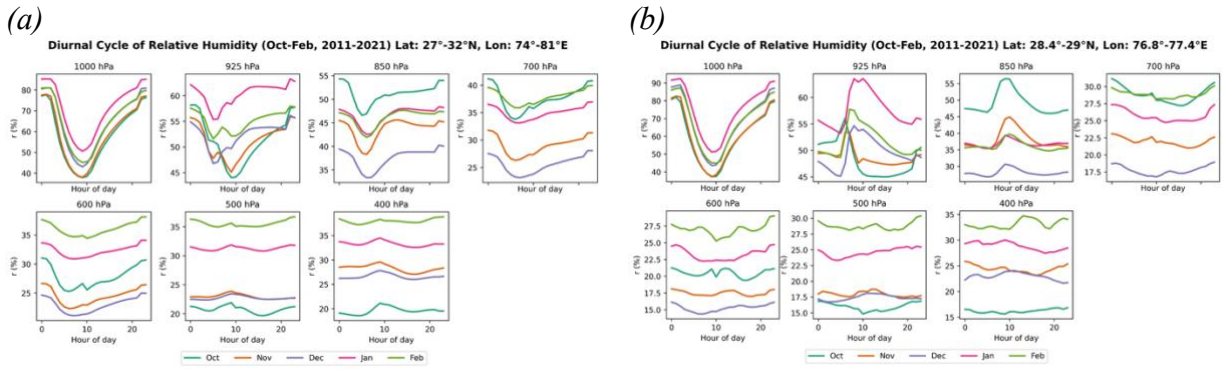

Figure 9: Mean diurnal cycle of RH for the winter months (October-February) from 2011 to 2021. The panels show the average daily pattern at various pressure levels for (a) the inner Delhi domain and (b) the broader outer domain. Each subplot corresponds to a specific pressure level, with colored lines representing the spatially averaged rh (in %) for each hour of the day.

The vertical profiles of relative humidity (Figure 10) exhibit a more intricate structure than those of other variables, characterised by alternating layers of moisture and dryness. Rather than showing a simple decrease with altitude, the profiles reveal a relatively moist boundary layer capped by a markedly drier mid-troposphere. Across all months, relative humidity is highest near the surface (1000-900 hPa) and decreases sharply to a minimum around 850 hPa. Above this dry layer, a modest recovery is often observed in the mid-troposphere (approximately 700-600 hPa).

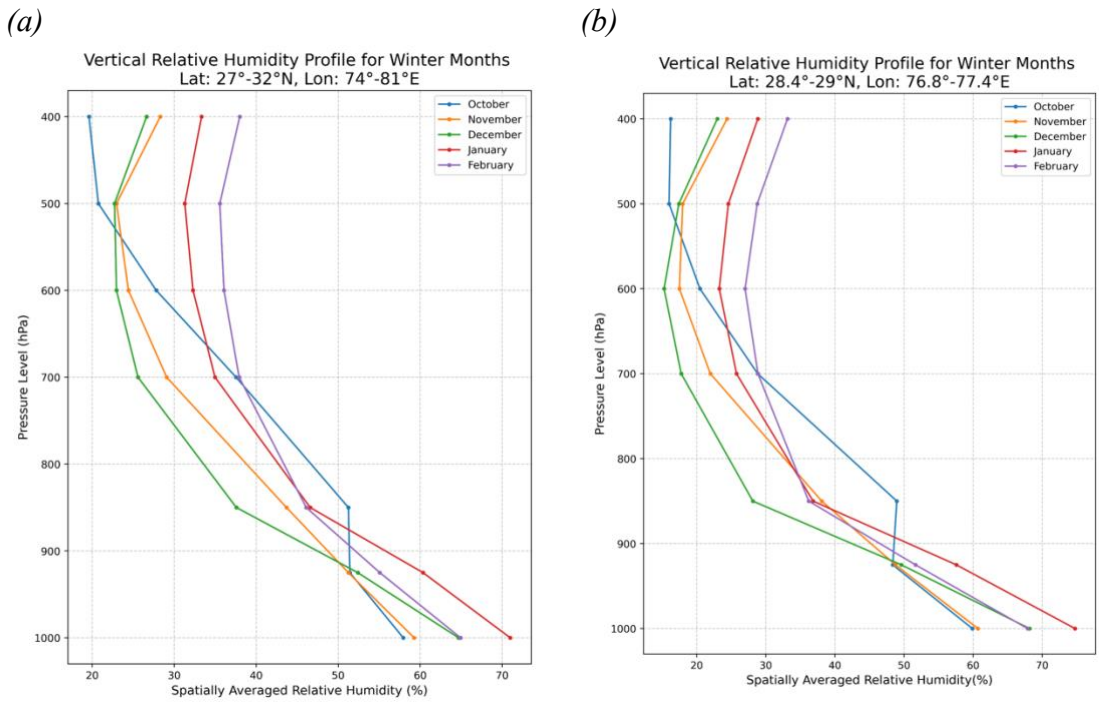

*Figure 10: Vertical profiles of spatially-averaged RH for winter months (2011-2021). The plots show the change in mean relative humidity (%) with pressure level (hPa) for (a) the broader outer domain and (b) the inner Delh*i domain.

This vertical configuration has important implications for the Saturation Check (RH > 80%) component of the MSI. The analysis indicates that at the key cloud-forming level of 850 hPa, the atmosphere is climatologically at its driest point within the lower troposphere. During the core winter months of December and January, the mean relative humidity at this level remains exceptionally low, typically between 40% and 55%. These values are well below the 80% threshold required for the formation of seedable clouds, clearly suggesting that the atmosphere is, on average, too far from saturation to support such operations.

1.3.2. Quantifying Potential Seeding Opportunities

Analysis of Rainfall Events and Seeding Suitability

A total of 137 rainfall events were found during the period of study. WD-induced rainfall events constituted 112 of the total rainfall events and the rest 34 were non-WD-induced rainfall events (Figure 11). This shows that during winter, the probability of rain without the influence of WD is

low. The mean of vertically integrated specific humidity (1000hPa- 300hPa) of rainy days was 29.98 kg/m^2 and 19.99 kg/m^2 for non-rainy days (Figure 11).

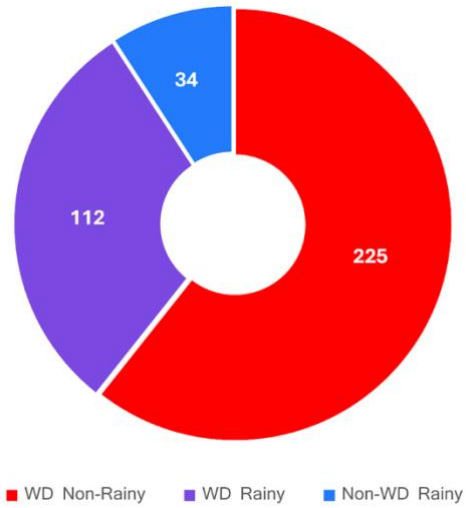

Figure 11: Pie chart showing the number of WD-induced and non-WD rainfall during the study period

To explore the suitable conditions for cloud seeding, non-rainy and light-rain days were analyzed for thermodynamic and cloud conditions. Thresholds for column-integrated specific humidity (q_{int}) and CC were defined as the 25th percentile values from all rainy days (Figs. 13-15). Days exceeding both thresholds were considered potentially suitable for cloud seeding. Using this approach, 92 days during the study period were identified as having moisture and cloud conditions comparable to moderate-to-heavy rainfall days (>7.5 mm). These days exhibit promising atmospheric conditions and therefore represent better opportunities for cloud-seeding interventions during winter compared to other non-rainy or light-rain days.

Number of Seedable Days in Each Month

This section quantifies the frequency of potentially "seedable" days by analysing the occurrence of cloudy days during the winter season. Using cloud fraction as a proxy for cloud cover, Figure 16 categorises the number of days meeting various cloud fraction thresholds (0.25, 0.5, and 0.75). The days are further classified based on the presence of a WD-the primary synoptic system for winter precipitation, whether rainfall occurred over Delhi.

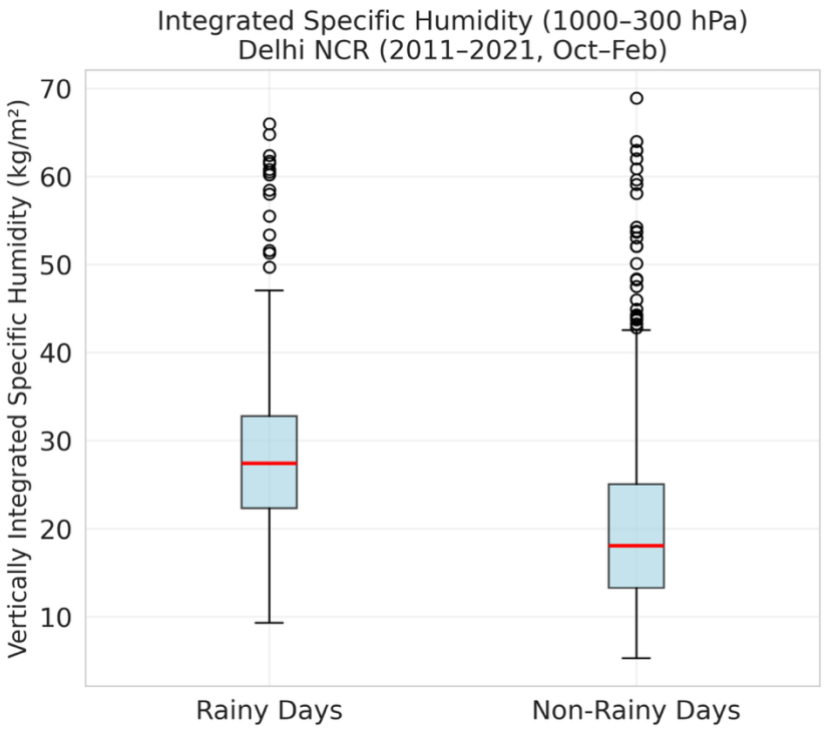

Figure 12: Vertically integrated specific humidity (kg/m^2) for rainy and non-rainy days

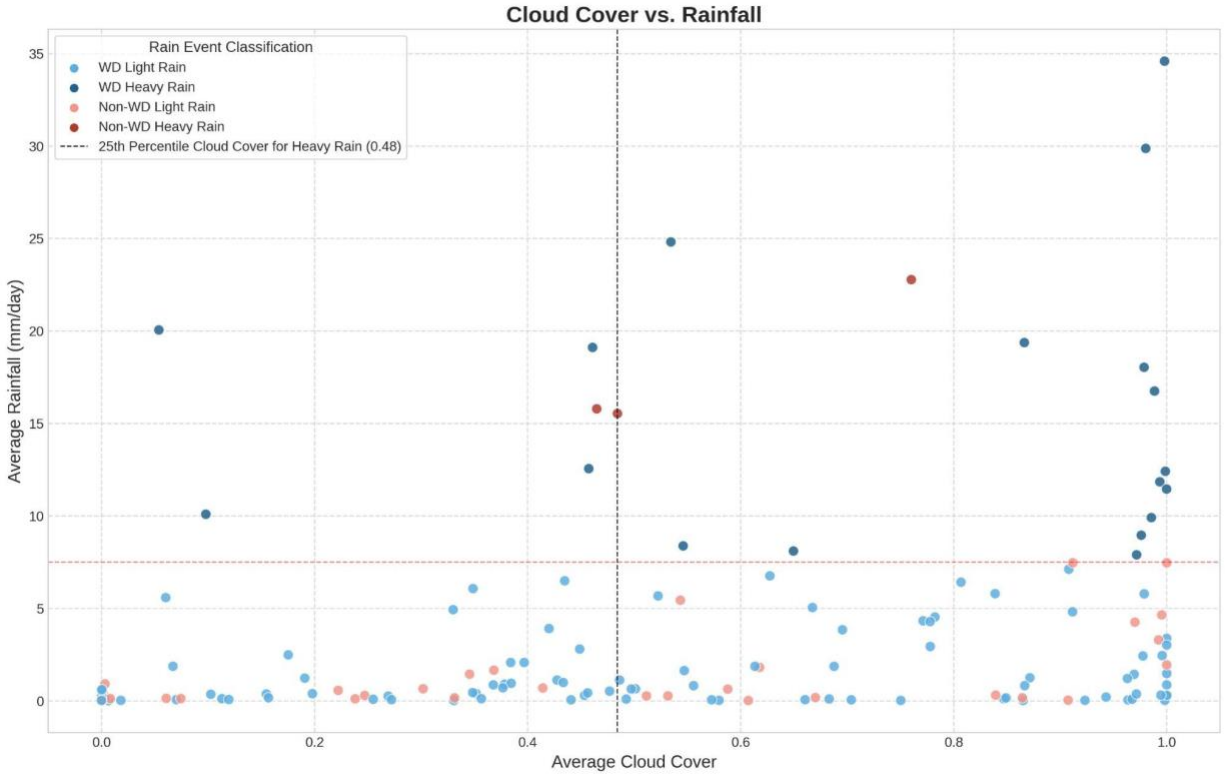

Figure 13: Scatter plot of rainfall vs average cloud cover fraction

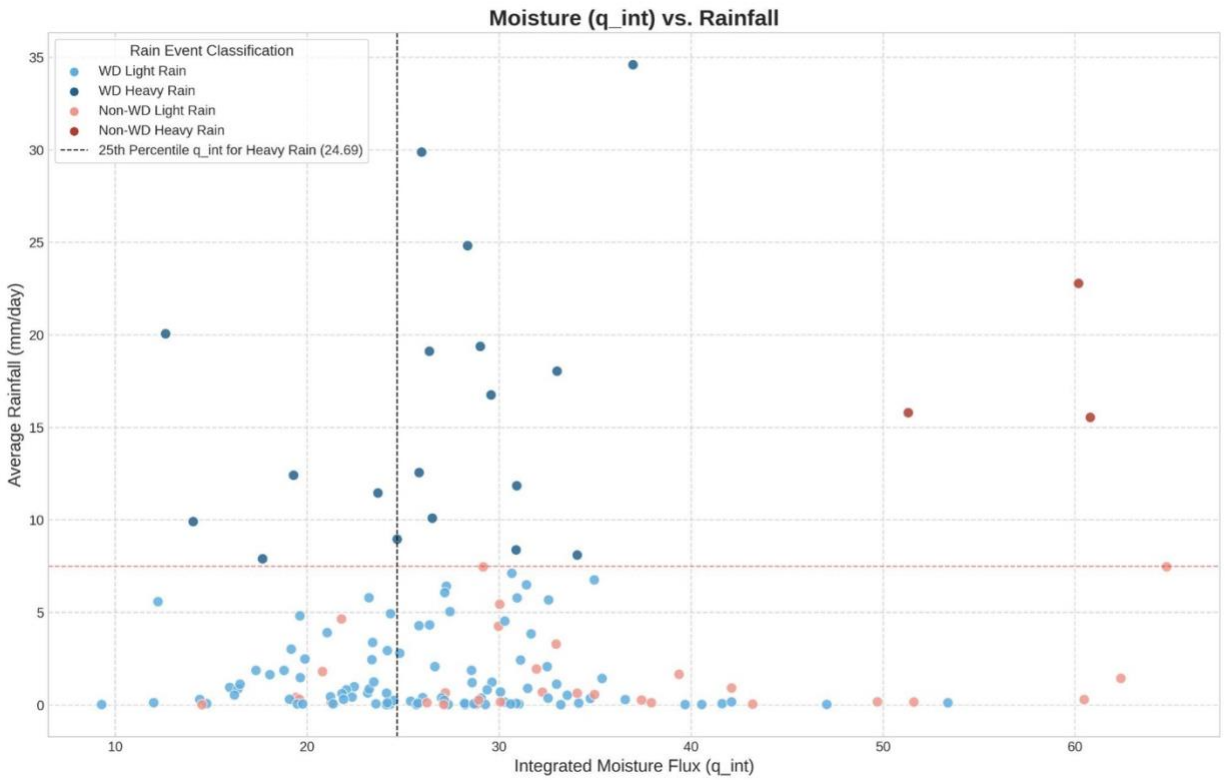

Figure 14: Scatter plot of moisture(q_int) vs rainfall

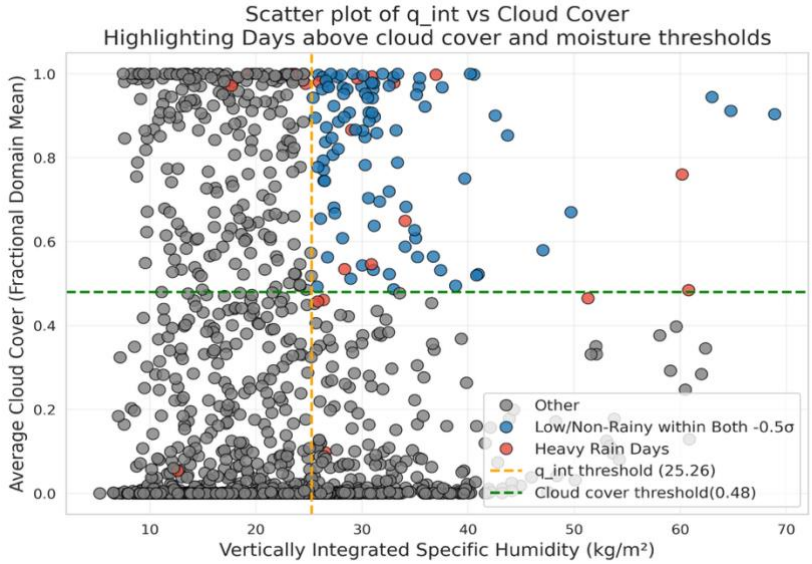

Figure 15: Scatter plot of moisture (q_int) vs average cloud cover fraction

The monthly distribution of cloudy days over Delhi reveals a distinct seasonal increase from October to February, peaking in January and February, and is strongly controlled by synoptic activity associated with WDs. Overall, while days with cloud fraction >0.25 are frequent (often >100 per month), the number decreases sharply at higher thresholds (0.5, 0.75), especially outside of active WDs. The analysis confirms WDs are the dominant mechanism for winter rainfall,

evidenced by the high number of rainy days during WD events (e.g., 38 in both Jan and Feb) compared to the infrequent non-WD rainy days. Conversely, the majority of cloudy but non-precipitating days occur without WD influence, representing periods of stable cloud cover. The most promising "window of opportunity" for cloud seeding lies within the "WD Day But No Rainfall" category; these days feature a dynamic, moisture-bearing system and cloud presence but lack natural rainfall. However, these opportunities are infrequent, with only 12 such days in December 17 in January, and 15 in February meeting the minimum cloud fraction threshold (>0.25) over the decade studied. This quantification aligns with the broader climatological analysis, indicating that ideal days for potential cloud seeding are not a common feature but rather a limited subset of specific synoptic events.

All

Month \ Cloud Fraction	0.25	0.5	0.75
Oct (310 days)	31	12	4
Nov (300 days)	67	19	10
Dec (310 days)	97	48	23
Jan (310 days)	146	81	22
Feb (283 days)	144	70	30

WD Day But No Rainfall

Month \ Cloud Fraction	0.25	0.5	0.75
Oct (39 days)	2	0	0
Nov (39 days)	9	2	1
Dec (50 days)	12	3	2
Jan (54 days)	17	3	0
Feb (43 days)	15	5	1

Not WD Day And No Rainfall

Month \ Cloud Fraction	0.25	0.5	0.75
Oct (253 days)	24	9	3
Nov (246 days)	51	16	9
Dec (239 days)	70	36	17
Jan (209 days)	88	53	13
Feb (192 days)	90	46	20

Not WD But Rainfall

Month \ Cloud Fraction	0.25	0.5	0.75
Oct (12 days)	4	3	1
Nov (3 days)	2	0	0
Dec (3 days)	2	1	0
Jan (9 days)	9	6	4
Feb (7 days)	7	3	3

WD Date And Rainfall

Month \ Cloud Fraction	0.25	0.5	0.75
Oct (6 days)	1	0	0
Nov (12 days)	5	1	0
Dec (18 days)	13	8	4
Jan (38 days)	32	19	5
Feb (38 days)	31	16	6

Figure 16: Number of days in each month when the cloud fraction was more than 0.25. The days have been further classified into days with cloud fraction thresholds of 0.25, 0.5, and 0.75. For all three subgroups the days have been divided based on Western Disturbance activity and associated rainfall over Delhi.

Assessment of Seeding Suitability with the MSI

This analysis applies the MSI to the categorised cloudy days, providing a quantitative assessment of truly seedable opportunities. The results distinguish between days that are merely cloudy and those that possess the deeper atmospheric conditions necessary for precipitation enhancement.

Figure 17 links MSI scores (1-4, representing met conditions met beyond cloud cover) with cloud fraction thresholds (0.25, 0.5, 0.75), categorised by WD presence and rainfall. Analysis reveals that under WD but no rainfall conditions, cloudy days are infrequent, peaking slightly in Dec-Feb,

and almost exclusively exhibit MSI=1, meaning only the cloud fraction threshold is met, with rare MSI=2 cases in Jan/Feb. Conversely, no WD and no rain conditions show much higher frequencies of cloudy days, especially in Jan/Feb, but these are dominated by MSI=1 and 2, indicating cloud formation under limited dynamic/thermodynamic support, with MSI > 2 being absent. The no WD but rainfall category represents very few, weakly organised events (MSI=1 or 2).

WD No Rain

Cloud Fraction	0.25				0.5				0.75			
MSI / Month	1	2	3	4	1	2	3	4	1	2	3	4
Oct												
Nov	2				1							
Dec	4				1				1			
Jan	3	2				1						
Feb	6				1							

No WD No Rain

Cloud Fraction	0.25				0.5				0.75			
MSI / Month	1	2	3	4	1	2	3	4	1	2	3	4
Oct	5				4				1			
Nov	4				2				1			
Dec	8	1			3				1			
Jan	27	1			17	1			7	1		
Feb	25	2			14	1			8			

No WD But Rain

Cloud Fraction	0.25				0.5				0.75			
MSI / Month	1	2	3	4	1	2	3	4	1	2	3	4
Oct	3				3				1			
Nov	1											
Dec	2				1							
Jan	2	1			2	1			2	1		
Feb	3				2				2			

WD Rainy

Cloud Fraction	0.25				0.5				0.75			
MSI / Month	1	2	3	4	1	2	3	4	1	2	3	4
Oct												
Nov	1											
Dec	8				5				3			
Jan	15	1			10	1			3	1		
Feb	12	4			6	4			3	3		

Figure 17: Number of days in each month with corresponding MSI (ranging from 1-4) classified into days with cloud fraction thresholds of 0.25, 0.5, and 0.75. For all three subgroups the days have been divided based on Western Disturbance activity and associated rainfall over Delhi.

Even the WD rainy category, while showing the highest cloud fractions (especially in Jan/Feb), mostly corresponds to MSI=1 and 2. This suggests that while WDs bring extensive cloud cover, the full suite of necessary meteorological conditions for high suitability is often not met simultaneously. Overall, winter cloudiness in Delhi predominantly occurs under weak to moderate atmospheric support (MSI $\leq$ 2), with WDs being the primary driver for widespread and dense cloud cover, particularly during rainy phases. Crucially, this confirms that the number of genuinely "seedable" days is extremely limited. Even when promising cloudy conditions coincide with a WD, the underlying atmosphere is frequently too dry or stable to meet the multi-faceted MSI criteria, reinforcing that viable seeding opportunities are rare, anomalous events rather than common features of Delhi's winter.

2. Role of Cloud Condensation Nuclei and Cloud Seeding Potential

2.1 Introduction

Delhi's persistent air pollution crisis presents a complex atmospheric challenge driven by high aerosol loading, urban emissions, and unfavorable meteorological conditions. Aerosols alter radiation balance and microphysical processes by acting as CCN, influencing droplet formation, cloud lifetime, and precipitation efficiency. During winter, the boundary layer remains shallow, trapping particulate matter and further elevating CCN concentrations. Understanding the interactions between aerosols, CCN, and clouds is crucial for determining the potential of cloud seeding as a rainfall enhancement and pollution mitigation strategy.

This section reviews cloud–aerosol interactions and seeding feasibility for Delhi using experimental and modeling studies from India and across the world. The objective is to assess whether artificially induced rain through targeted cloud seeding could promote wet scavenging of pollutants and reduce airborne particle concentrations in Delhi's atmosphere.

Recently, IIT Kanpur and IMD announced a plan to run a cloud seeding experiment as a trial for addressing the severe air pollution in Delhi-NCR during October 2025. They propose to use modified Cessna aircraft 206H using flares mixed with Silver Iodide (AgI), powdered rocksalt and iodised salt. It is hypothesised that this mixture facilitates cloud drop formation by triggering the formation of Ice crystals on AgI. Trial runs of aircraft are proposed to fly over an area of 100 sq km for about 5 times each lasting about 90 minutes at a height of about 10000 ft, targeting nimbostratus clouds with moisture content >50%. It is estimated to cost about Rupees 1 crore for one mission. This report in view of this proposal is an attempt to explore whether there are enough clouds for successful seeding, why AgI is important, and the implications of such an experiment for the environment of a polluted Delhi during the dry winter season.

Precipitation in clouds happens when the pull of gravity overcomes the buoyancy of cloud droplets or ice crystals, which can only happen after sufficient droplet/crystal growth. AgI, particularly used in seeding cold clouds to induce rain, as proposed to be the case here, boosts the droplet/ice crystal formation in clouds. Cloud seeding has been successfully attempted to increase precipitation and/or hail suppression in some trials while only a few trials have been done to

mitigate pollution through wet scavenging. The earliest use of cloud seeding for strategic (Operation Popeye in Vietnam) and disaster management purposes (Project Stormfury) was reported by the United States, the latter of which was deemed a failure.

The dominant meteorological and thermodynamic variables controlling cloud formation and the success of a seeding event are moisture content, availability of CCN, and strong updraft velocities. The major criticism against cloud seeding is its feasibility and efficiency for large-scale implementation with CCN injection into small point sources, particularly in cold cloud conditions. Most mixed-phase or cold clouds don't have ice crystals above -12 °C, hence natural ice nuclei (IN) are not sufficient, and weak updrafts in wintertime add further problems. CCN activation and cloud formation is very sensitive to the initial conditions of the thermodynamic, radiative, and aerosol properties, which make this system non-linear with competing feedback mechanisms. The complex cloud structures coupled with how aerosols change their behaviour near clouds and with varying meteorological conditions, makes it difficult to establish proper causal chains involved in cloud seeding with available statistical tests and modeling methods.

2.1.1 Cloud Condensation Nuclei (CCN)

CCN are aerosol particles that initiate droplet formation under supersaturated conditions. Their number concentration, composition, and size distribution determine the cloud droplet number concentration (CDNC) and influence precipitation formation. The Twomey effect explains that higher CCN concentrations produce smaller droplets, enhancing cloud albedo but suppressing warm rain initiation. Over Delhi, elevated aerosol levels from vehicular and biomass sources lead to enhanced CCN, forming numerous small droplets less capable of coalescence. This delays precipitation and results in thicker, longer-lived clouds (Koren et al., 2005).

Clouds in polluted regions are more vigorous in convection owing to a combination of suppression of early rainout of cloud and its stabilisation with suppression of freezing and release of latent heat at higher altitude. Aerosol perturbations cause secondary convection, which is observed mostly in warm clouds. Generally, if there are high amounts of aerosols, more invigoration is expected as CCN can be higher and thus increases the formation of small cloud drops, which in turn increases the collision and coalescence process and thus resulting in rain. Even if the atmosphere is cleaner, large drops can form, overcoming the updrafts and precipitate later. Polluted clouds are less likely to form warm precipitation as these clouds last longer, and drops can go even higher increasing cloud top height. Above the freezing level, if ice-nucleating particles are scarce, heterogeneous

ice nucleation remains inefficient, allowing supercooled droplets to persist and thereby delaying precipitation.

Observational evidence supports aerosol invigoration of convection, where polluted environments with elevated CCN produce stronger updrafts and taller clouds. However, excessive aerosol loading can suppress rainfall entirely by inhibiting droplet growth. Such microphysical dynamics define the baseline for evaluating cloud seeding effectiveness in Delhi's atmosphere.

2.1.2 Theoretical Background and Cloud Microphysics

The Köhler theory explains droplet activation as a balance between solute effect and curvature effect. Kaplan's microphysical framework provides a dynamic perspective on vapor pressure, droplet growth, and supersaturation. In polluted regions, smaller hygroscopic particles dominate, leading to high CCN counts but reduced droplet size. Consequently, the collision-coalescence process weakens, delaying warm rain. In contrast, larger Giant CCN (GCCN) enhance droplet growth and early precipitation formation. Thus, cloud seeding introduces artificial GCCN or IN to compensate for natural rain suppression.

Cloud Seeding Mechanisms

Cloud seeding involves the deliberate introduction of nucleating agents to stimulate precipitation. It includes two primary approaches: hygroscopic seeding (warm clouds) and glaciogenic seeding (cold clouds). Hygroscopic seeding uses salts such as NaCl or KCl below cloud base to promote droplet coalescence, while glaciogenic seeding employs silver iodide (AgI) particles to initiate freezing near cloud tops. The effectiveness depends on parameters such as cloud liquid water content, vertical velocity, and updraft structure.

Globally, seeding experiments have shown varying success rates. Israel's long-term program reported rainfall enhancement of 13-16%. China's dynamic and static seeding programs improved snowfall and rainfall formation. In contrast, Thailand's randomized trials achieved limited statistical significance but indicated positive local effects. UAE's missions showed increased PM10 concentrations due to residual AgI. Meanwhile, the Korean and Australian experiments demonstrated fine-dust reduction and increased precipitation under specific synoptic conditions.

Global Studies:

Table 1. Global studies

	Place	Time period	Method	Remarks
1	United Arab Emirates (UAE)	Jan-March 2017	Glaciogenic seeding (AgI)	The PM10 and PM2.5 data showed a significant increase in PM10 concentrations during Jan–March 2017, when the cloud mission occurred, compared to the months thereafter. The AgI crystals fired into the clouds but failed to take part in any nucleation process eventually fell down while degrading into smaller particles forming PMs of different sizes that may be suspended and float in the atmosphere (Malik et al. 2018)
2	Northern Israel	Since 1975	Glaciogenic Seeding (AgI)	Enhanced rainfall there by 13-16% (Gagin and Neumann 1981)
3	Wyoming	2007-2010	Glaciogenic seeding (AgI)	AgI seeding could produce additional precipitation in winter orographic clouds (Huggins, 2009)
4	NW Thailand	April-May-June 1994-1998	Glaciogenic seeding	This experiment did not reach statistical significance in the time allotted to it. Thus, this experiment did not "demonstrate" or prove the efficacy of glaciogenic cloud seeding in this context. The confidence interval analyses suggest there is 72% confidence that there was a positive effect of seeding on cells, 79% confidence that there was a positive seeding effect on units, but only 20% confidence that there was a positive effect on cells and units when considered jointly.
5	West Korea	November 2020	Hygroscopic seeding	The average concentration of cloud, drizzle, and precipitation particles increased after seeding as compared with the observations before and during seeding. (aircraft data) Cloud seeding was found to be effective for reducing fine dust concentration.

6	China	1997-2007	Glaciogenic seeding	Glaciogenic cloud seeding has 2 approaches, 1) static seeding, which focuses on cloud microphysical processes, and is used to create ice crystal particles and enhance snow and graupel production by increasing the number of ice particles and triggering precipitation processes earlier in the lifetime of the cloud. 2) dynamic seeding, which increases the buoyancy of the cloud by converting supercooled liquid drops to ice.
7	Idaho	Jan-March 2017	Glaciogenic seeding	In some cases, the experiment detected zigzag lines of reflectivity in radar data that corresponded with the seeded material, and in-situ measurements showed changes in the cloud's microphysical properties. Researchers are continuing to analyze the data to quantify the amount of additional snowfall produced by seeding and determine the conditions under which seeding is most effective.

Indian Studies:

Table 2. Indian studies

	Place	Time period	Method	Remarks
1	Karnataka	Aug-Nov 2017 (Varshad hare)	Hygroscopic seeding	Unique rainfall data at high spatial (5 km) and temporal (15 min) resolution First time the response of seeding in terms of increase in rainfall at the ground Enhancement of rainfall due to seeding by floating control-target area rainfall Mean increase in rainfalls due to hygroscopic and glaciogenic was ~12 and 19.9 mm. The average increase of 27.9% at Taluk level rainfall above the natural rainfall (618 events)

2	Solapur, Maharashtra (CAIPEEX IV)	Monsoon period for 2018 and 2019	Hygroscopic seeding	Rainfall can be enhanced by up to ≅ 46±13 % at some locations and on average, ≅ 18±2.6 % in 100 square kilometers area in the downwind of seeding location. Contributed to ≅ 867 million liters of water, yielding a positive cost-benefit ratio.

Some Modelling studies:

Table 3. Modelling studies

	Study	Citation	Major findings
1	A mathematical model for the removal of pollutants from the atmosphere through artificial rain	Tripathi, A., Misra, A. K., & Shukla, J. B. (2021). A mathematical model for the removal of pollutants from the atmosphere through artificial rain. Stochastic Analysis and Applications, 40(3), 379–396. https://doi.org/10.1080/07362994.2021.1915802	The nonlinear mathematical model is analyzed in the presence of white noise and proved that if rain persists, the pollutants can be totally washed out. It has been observed that the environmental disturbances are not much favorable in such experiments as the presence of environmental disturbance may destabilize the system. It is found that to remove pollutants completely, it is necessary to prevent the formation of pollutants. The simulation is performed to support the analytical findings.

2	Assessment of Possible Precipitation Enhancement by Glaciogenic Cloud Seeding Using WRF: A Case Study	Pourghasemi, M.A., Memarian, M.H. & Zare, A. Assessment of Possible Precipitation Enhancement by Glaciogenic Cloud Seeding Using WRF: A Case Study. Russ. Meteorol. Hydrol. 47, 553–560 (2022). https://doi.org/10.3103/S1068373922070 10X	The successful rate of cloud seeding operations greatly depends on the local atmospheric condition, such as temperature and water vapor at the most appropriate height on this experimental day. As a result of increasing the number of aerosols at the SEED simulation the cloud cover is increased, water vapor mixing ratio is decreased, and updrafts and downdrafts become more intense and frequent. That provides favorable conditions for more rainfall. However, the increase in IN, in a result of seeding, has different effects on the simulated region
3	The effects of giant CCN on clouds and precipitation: A case study from the Saudi Arabia program for the assessment of rainfall augmentation	Teller, Amit & Axisa, Duncan & Breed, Daniel & Bruintjes, Roelof. (2008). THE EFFECTS OF GIANT CCN ON CLOUDS AND PRECIPITATION: A CASE STUDY FROM THE SAUDI ARABIA PROGRAM FOR THE ASSESSMENT OF RAINFALL AUGMENTATION.	Used the measured data in two similar cloud models in order to compare their performances in one particular scenario. In polluted environment where aerosol concentration in large, additional GCCN may increase the total precipitation while in clean case where the aerosol loading is low, additional GCCN reduced the total precipitation due to the reduced amount of water vapor in the mixed phase region of the cloud as precipitation starts earlier in this case injecting hygroscopic material to the cloud, as part of cloud seeding, in order to increase the concentration of GCCN might have a negative effect on precipitation in certain conditions where it may speed up the formation of large droplet in the warm regions of the cloud while it prevents much of the water vapor to reach higher altitude so graupel and ice production will be suppressed.

4	Assessing glaciogenic seeding impacts in Australia's Snowy Mountains: an ensemble modeling approach	Chen, S., Xue, L., Tessendorf, S. A., Chubb, T., Peace, A., Kenyon, S., Speirs, J., Wolff, J., and Petzke, B.: Assessing glaciogenic seeding impacts in Australia's Snowy Mountains: an ensemble modeling approach, Atmos. Chem. Phys., 25, 6703–6724, https://doi.org/10.5194/acp-25-6703-2025, 2025.	Simulated seeding efficacy highly depends on meteorological conditions. Stratiform cases exhibited consistent precipitation enhancement, while convective cases showed reductions and downwind shifts in precipitation. Cases, with deep, convective clouds and active precipitation processes, are considered the least ideal for cloud seeding.

2.3 Data and Methods

The methodology integrates observational and literature-based synthesis. Koren et al. (2010) analysed cloud properties by dividing AOD into different regimes (low, medium and high), and the same approach is followed here. Cloud climatology parameters such as cloud base height, cloud fraction, and liquid water content (2011-2021) were analyzed against different AOD bins. Vertical aerosol optical depth profiles were also examined to infer CCN variations.

Table 4. Datasets

Data sets used	**Time period**	**Resolution (lat x lon)**
ERA5 Cloud cover	2011-2021	0.25°x0.25°
ERA5 Cloud base height	2011-2021	0.25°x0.25°
ERA5 Cloud type	2011-2021	0.25°x0.25°
CALIPSO vertical distribution of AOD	2011-2021	333m
MERRA2 AOD	2011-2021	0.5°x0.625°
Ceilometer (IITD-Sonipat Observatory)	2021-2022 (1 day for each month - ONDJF)	-

2.4 Results

Vertical aerosol profiles

CALIPSO data is used to look at the vertical aerosol profiles over the Delhi region (Figure 18). High values of the backscatter coefficient in the lower atmosphere (below 2km) indicate the aerosol layers. This finding is corroborated by data from instruments at the IITD-Sonipat Observatory. Ceilometer backscatter coefficients and depolarization ratios show similar aerosol layers confined close to the surface.

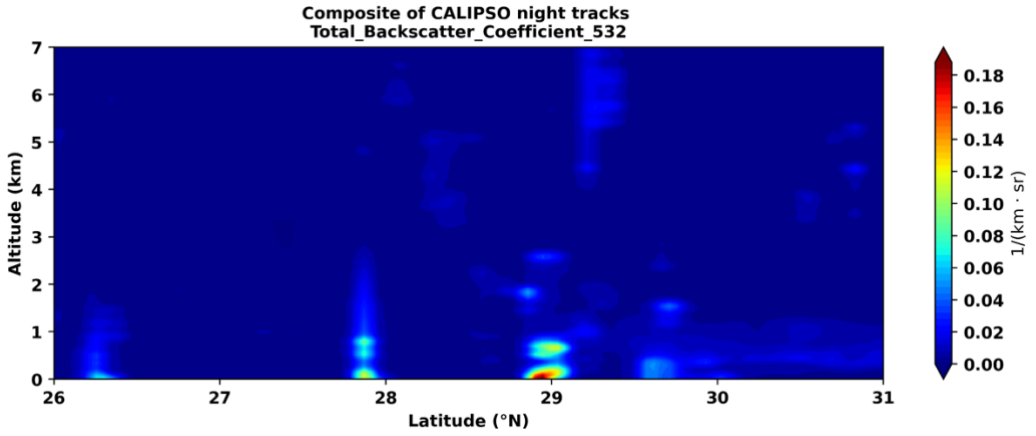

Figure 18: Composite vertical profiles of the total backscatter coefficient at 532nm using night tracks (14 passes) from the CALIOP instrument.

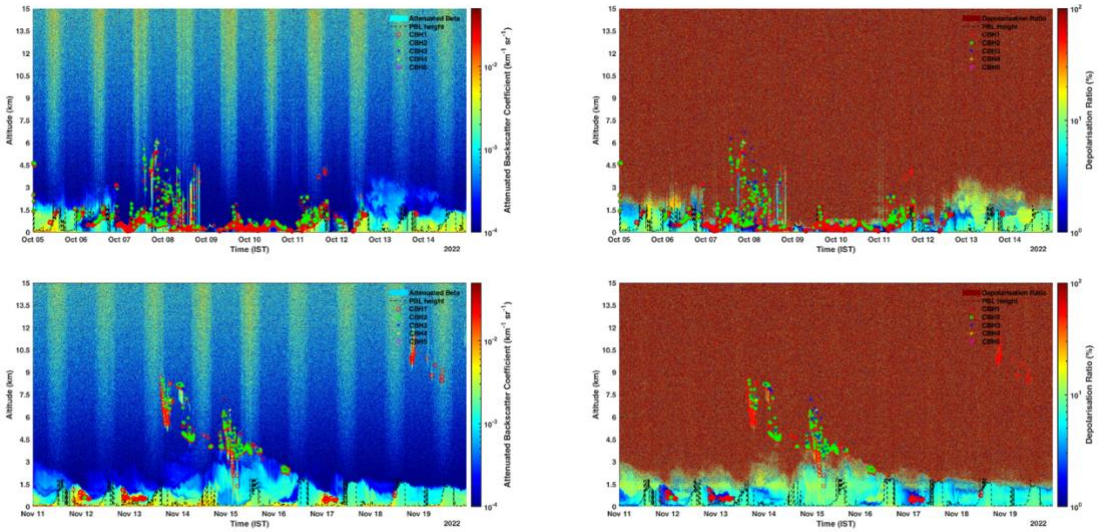

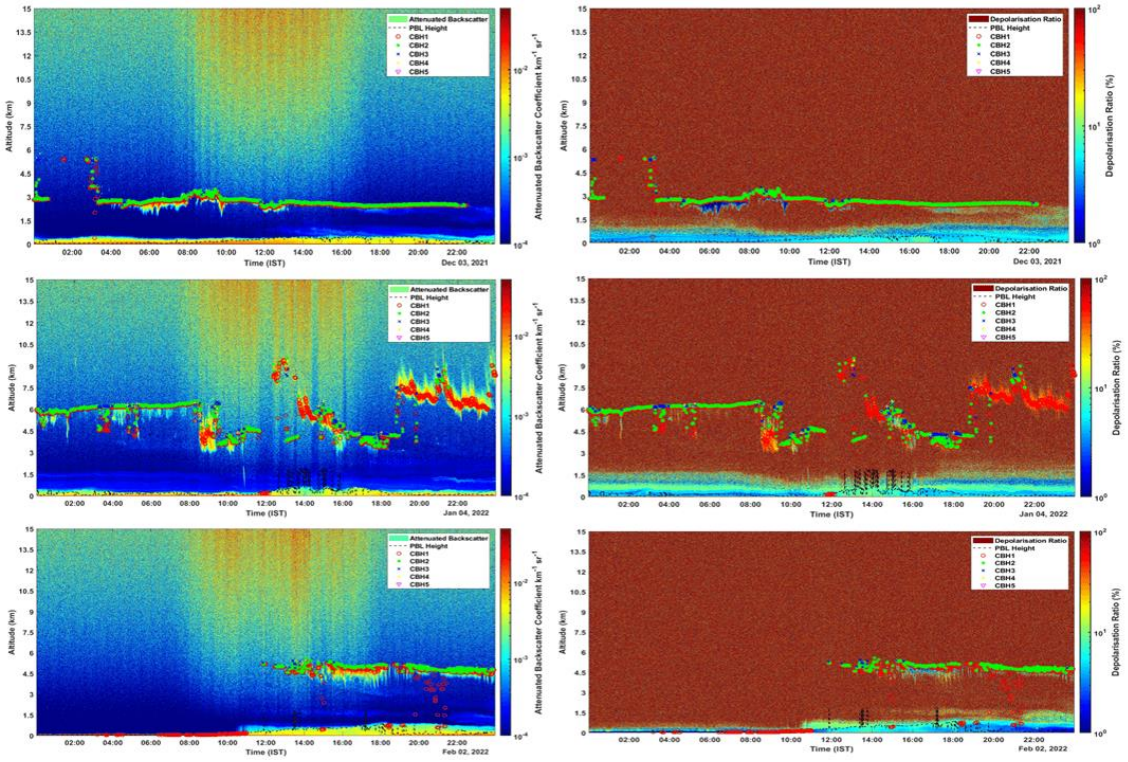

Figure 19: Data from the ceilometer at the IITD-Sonipat Observatory showing one day for each month from October 2021 to February 2022 in order. The left panels show the backscatter coefficient, and the right panels show the depolarization ratios. October and November have higher cloud layers. The higher backscatter coefficient around 3km in the Dec-Feb months indicates the presence of cloud layers, while that near the ground suggests aerosols are confined close to the surface.

Cloud occurrence frequency

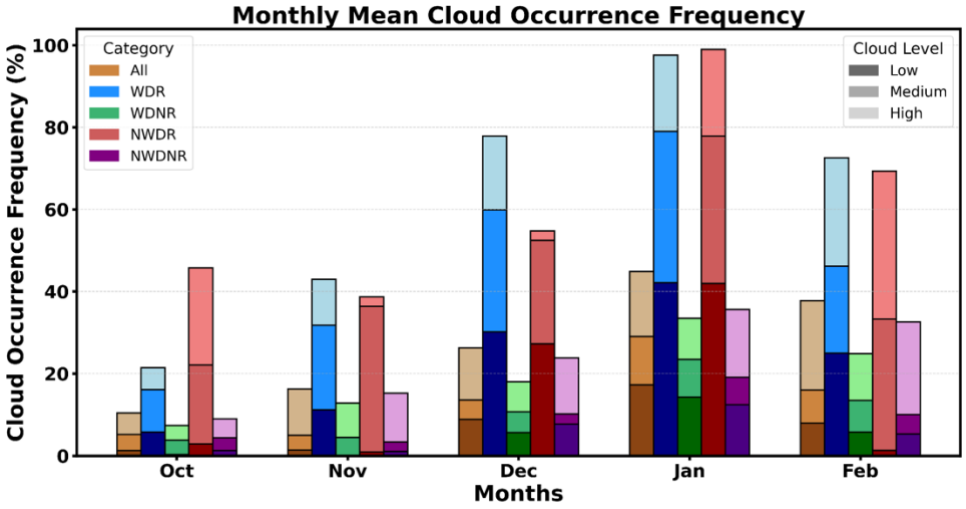

Figure 20: Cloud occurrence frequency for each category, month-wise. It is highest for the Western Disturbance rainy days and non-Western Disturbance rainy days, which is to be expected. The DJF winter months have a greater number of WDs than the ON months, which is reflected in the occurrence frequency as well. (WDR - Western Disturbance Rainy Days, WDNR - Western Disturbance Non-Rainy Days, NWDR - Non-Western Disturbance Rainy Days, and NWDNR - Non-Western Disturbance Non-Rainy Days).

Cloud cover by AOD bins

Figure 21 shows the total cloud cover and cloud base height distributions by AOD bins. We divide the AOD into three bins - Low (0-0.15), Medium (0.15-0.35) and High (>0.35). This classification is based on Fan et al. (2009). Both rainy day categories (WDR and NWDR) do not have any days in the low AOD category. a) Cloud cover is generally less in the dry winter months over the region. All three AOD categories show less than ~30% cloud cover for most day types. The 2 outliers noted here are the greater fraction for NWDR days in both the medium and high regimes, and for WDR in the high AOD regime. b) Cloud base height can indicate the Lifting Condensation Level/Convective Condensation Level (LCL/CCL). The cloud base height here shows an inverse relationship with the aerosol loading, showing higher values for lower aerosol loads. The low aerosol regime shows cloud base heights around 7-8km, with WDNR levels going even above 10km, while the high aerosol regime shows cloud base heights below 4km. However, there is no clear pattern that emerges amongst the different day types.

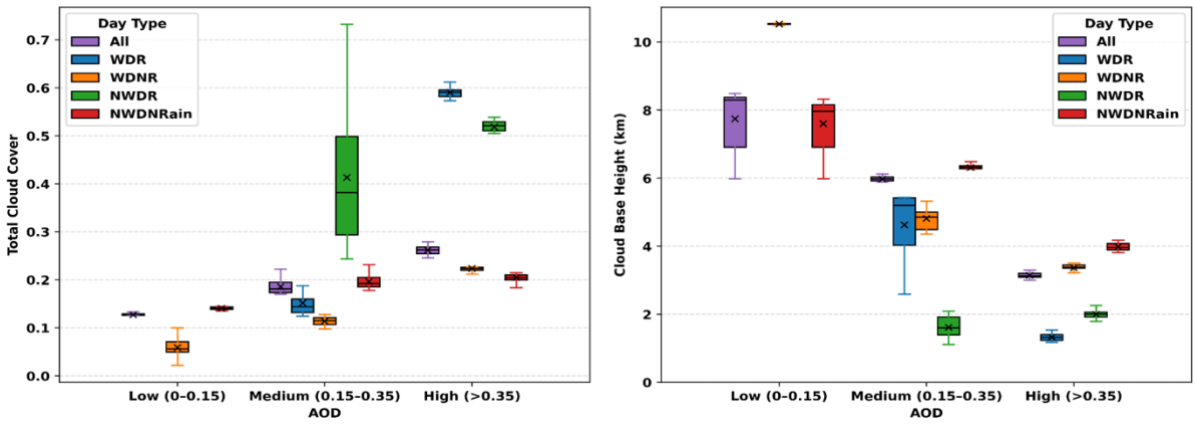

Figure 21: Total cloud cover and cloud base height distributions by AOD bins.

Cloud liquid/ice water by AOD bins

Both show higher values predictably for the rainy days, especially for the high aerosol loading (which implies higher CCN). Non-WD rainy days show higher values for both variables in the medium AOD regime as well, which is not observed for the WD rainy days. Low cloud cover in the low aerosol regime translates to very low values of liquid/ice water.

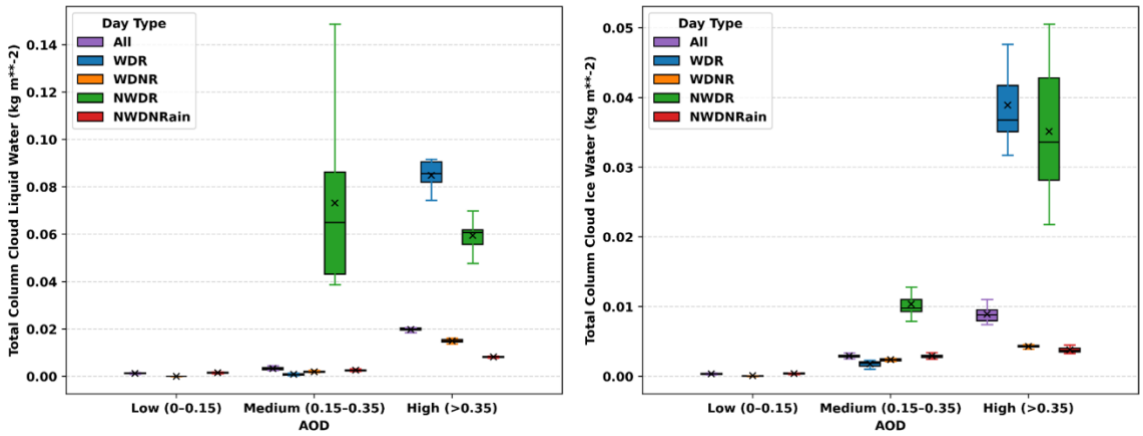

Figure 22: Same as Figure 21 but for total column liquid and ice water.

Cloud types by AOD bins

The type of clouds observed (low, medium and high) are also analysed using the ERA5 dataset. The dataset defines low clouds as having a cloud base height (CBH) from the surface up to 2 km, medium clouds are from 2 km to 6 km, and high clouds are above 6 km. Cloud cover in general remains low (less than ~35%) and rainy days (both WDR and NWDR) experience much more clouds, especially the low and medium types, than non-rainy days, which is to be expected.

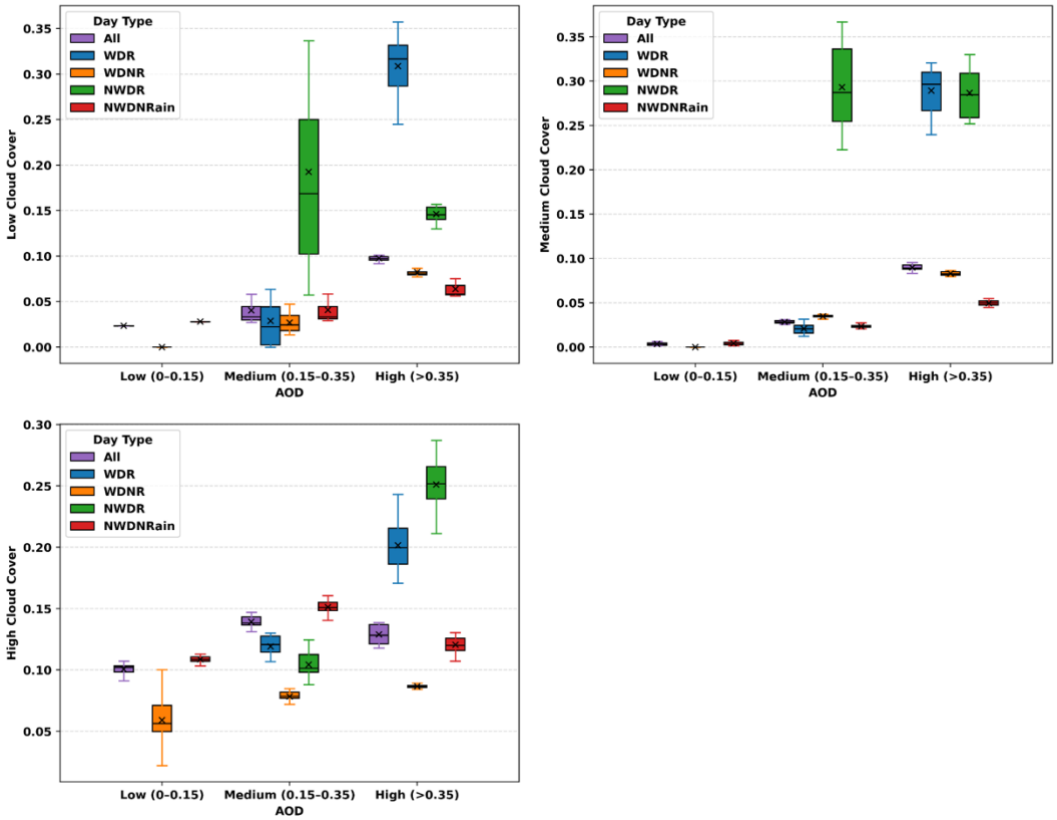

Figure 23: Same as Figure 21 but for the low cloud cover, medium cloud cover and high cloud cover respectively.

The analysis reveals that the winter months in Delhi tend to have aerosols concentrated close to the surface, which can be explained by the low height of the boundary layer. Cloud cover remains low (<30%) throughout and increases only during WD and non-WD rainy days, as expected. Cloud cover also shows an inverse relationship with AOD; the highest fractions are observed over the high AOD regime. No clear pattern emerges for the cloud base height.

Based on a review of existing literature, cloud seeding seems to be possible when pre-existing conditions of rain are present, as determined by meteorological and thermodynamic variables. Provided that rain conditions exist, ice water is notably higher only at high AOD bins, indicating that ice nucleation processes are favored during high AOD days, which can serve as a proxy for the availability of more CCN and secondary convection, as discussed theoretically.

3. Pollutant Removal Efficiency and Post-Rainfall Recovery Dynamics

3.1 Introduction

The Indo-Gangetic Plain (IGP) remains one of the most polluted regions in India, with NCR frequently reporting wintertime PM2.5 levels exceeding 300 $\mu g/m^{3,}$ nearly 20 times the WHO guideline (Guttikunda and Calori, 2013). Persistent emissions from traffic, industries, construction, biomass burning, and dust, combined with weak dispersion and strong temperature inversions with low boundary layer height, create severe pollution episodes. Due to anthropogenic activities from various emission sectors are formed secondary inorganic aerosols (sulfate, nitrate, ammonium or SNA) dominate fine-particle mass concentration, contributing up to 70 % of PM2.5 during stagnant conditions (Tiwari et al., 2015), while mineral dust, organics, and black carbon further enhance the regional aerosol burden (Gani et al., 2019). Despite policy interventions such as the Graded Response Action Plan, air quality improvements remain episodic, underscoring the need for rapid, short-term mitigation strategies during extreme pollution events (UNDP report, 2024).

Rainfall is a natural mechanism for atmospheric cleansing, removing aerosols and soluble gases through in-cloud and below-cloud scavenging (Seinfeld and Pandis, 2016). Empirical and modeling studies report 10 to 40% reductions in PM during rain, depending on droplet size, intensity, and aerosol composition (Maria et al., 2005; Lu et al., 2019; Jones et al., 2022). Hygroscopic and coarse particles such as sulfate, nitrate, and dust are most efficiently removed, whereas hydrophobic black carbon and organics show weaker scavenging (Hegg et al., 2011). However, observed improvements are transient: concentrations often return to pre-event levels within 24 - 72 hours due to persistent emissions and boundary-layer recovery (Fujino et al., 2022; Zhao et al., 2020).

Cloud seeding, which aims to enhance rainfall by stimulating droplet formation and coalescence, could theoretically amplify this cleansing process. India's CAIPEEX program (CAIPEEX report, 2023) has demonstrated rainfall increases of 18 - 46% through hygroscopic and glaciogenic seeding, but its potential to mitigate air pollution remains unexplored. The complex aerosol mixes and meteorological heterogeneity of Delhi–NCR make it an ideal yet challenging testbed to assess whether induced precipitation can meaningfully reduce particulate and gaseous pollution.

Rain removes aerosols via in-cloud nucleation scavenging and below-cloud impaction scavenging, with a clear size dependence. Using the scavenging amount mode framework, Wang et al. (2021) showed that the rain-rate bins contributing most to removal are ~10-12 mm/day (Aitken), 8-9 mm d^{-1} (accumulation), and 7-8 mm d^{-1} (coarse), and that rainfall frequency-not peak intensity-governs climatological wet removal. Convective precipitation, with larger drops, tends to remove submicron particles more effectively at 0.3-20 mm/day, while stratiform rain more efficiently scavenges coarse particles. However, rainfall is not a lasting solution for ultrafines (PM1; Particulate Matter with aerodynamic diameter ≤ 1 μm). Direct washout is weak, and Zhao et al. (2023) showed a compensating pathway: by clearing pre-existing surface area, rain lowers the condensation ($\Delta CS \approx 4\times10^{-2}\ s^{-1}$) and coagulation sinks ($\Delta CoagS \approx 1.5\times10^{-4}\ s^{-1}$), enabling new particle formation within ~1–60 h post-rain. Such events can supply 15-80% of N_{13-100} and up to ~47% of PM2.5 mass, replenishing fine particles. Overall, rain yields transient PM reductions unless paired with precursor emission controls.

3.2 Data and Methods

3.2.1. Air Quality Data

We collected open-source real-time air quality data for Continuous Ambient Air Quality Monitoring Stations (CAAQMS) available as on October 12, 2025 from the Central Pollution Control Board (CPCB; https://airquality.cpcb.gov.in/ccr/#/caaqm-dashboard-all/caaqm-landing). We consider data for five criteria air pollutants and meteorological parameters: particulate matter PM2.5 and PM10, Sulfur dioxide (SO_2), Nitrogen Oxides ($NOX \approx NO + NO_2$), and ozone (O_3), wind speed and wind direction at 1-hour resolution for the five-year period, 2017-2024. We considered a total of 5 sites out of 81 available sites (Fig. 3.1) within the Delhi NCR region for our study domain. The selected sites were filtered based on the criterion of having more than 80% data availability for each primary (SO_2, NOX) and secondary pollutant (PM2.5, PM10, O_3) for every year between 2017 and 2024, addressing the persistent data quality issues in the CAAQMS dataset (Figure 24). In terms of data availability, more monitoring sites became operational after 2019, whereas earlier years exhibited significant data gaps and a limited number of sites. Our data selection criteria focused on the most recent 8-year period (2017-2024) of available data (Figure 25). We further categorised the selected sites based on their land-use characteristics, including dense urban, industrial, green space, residential, and peri-urban areas (Table 5).

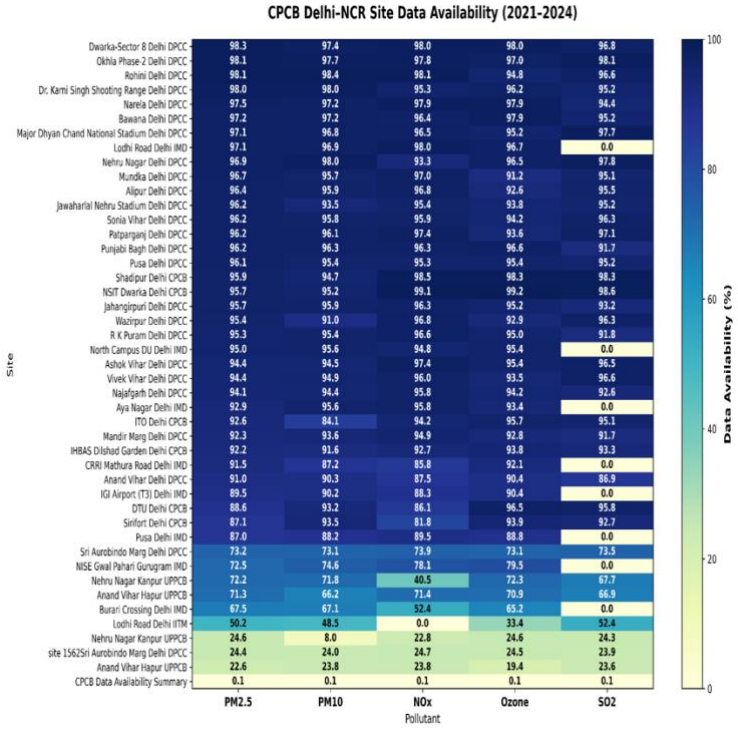

Figure 24: Availability of CPCB data (in percentage) for different criteria pollutants (PM2.5, PM10, NOX, O_3, SO_2) for different stations in the Delhi NCR Region.

Figure 25: Availability of CPCB data (in percentage) for different species (PM2.5, PM10, NOX, O_3, SO_2) for selected stations in the Delhi Region.

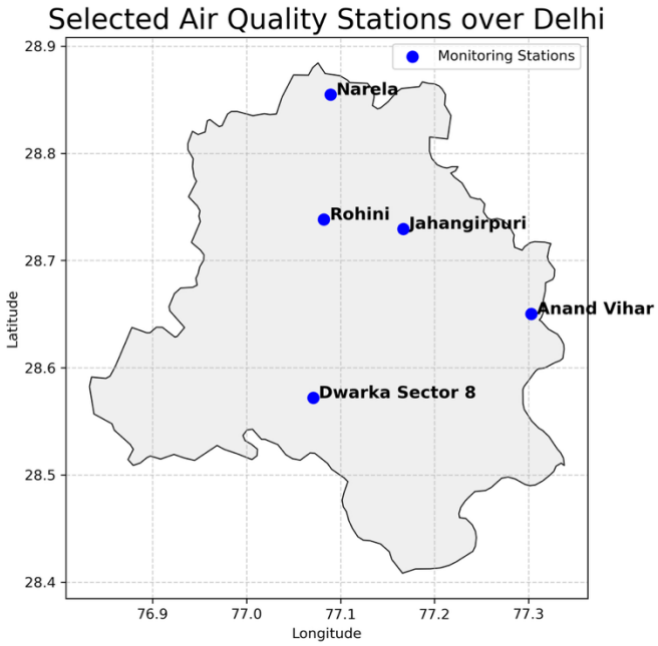

Figure 26: Locations of the selected air quality monitoring sites across the Delhi region.

To enhance the robustness of the air quality data preprocessing, we adopted widely used statistical approaches for identifying and removing outliers. Outlier detection and removal were carried out following the methodology proposed in the previous studies, which defines valid data within the 5th and 95th percentile range of the distribution. Data values outside this range were considered outliers and excluded from further analysis.

Table 5: Details of selected stations and respective land use land cover type

STATION	TYPE
Anand Vihar	Dense urban/Traffic Corridor
Jahangirpuri	Dense urban/ Residential
Dwarkar sector-8	Residential Colony
Narela	Suburban and Peri-urban
Rohini	Residential Colony

To analyze the effect of rainfall on particulate matter concentrations, AOD from MERRA-2 of resolution 0.5° x 0.625° was selected as a proxy. The day of rain was considered as t_0 and the AOD time series was plotted for the period t0-5 to till the AOD value reaches pre-rain 5 day mean for those rainfall events (WD and non-WD) with no other rainy days within the period of t_0-5 to

t_0. Welch's t-test was used to determine whether the reductions in AOD were statistically significant after the rain.

The climatology of winds was calculated for all days when WD tracks (both rain-inducing and dry) were present within the 10° box. The days of dry WD influence on wind speeds were identified as those with wind speeds greater than the climatological wind speed. The day of maximum influence (t_0) for each dry WD was defined as the day with the maximum wind speed over Delhi during its passage through the box. The AOD time series was also plotted for the period from t_0–5 until it returned to the pre-event five-day average. Welch's t-test was used to find whether the changes in AOD were statistically significant after t_0.

To quantify the immediate and lasting impact of rainfall on air quality, two key metrics were calculated for each event. The % Washout measures the direct cleansing efficiency of a rain event, calculated as the percentage change between the pollutant concentration on the day before the rain and the day after ((Pre-Rain concentration - Post-Rain concentration) / Pre-Rain concentration * 100). A higher positive percentage indicates a more effective removal of that pollutant from the atmosphere. Following this initial cleansing, the Recharge time was estimated to determine how long the beneficial effects lasted. This was calculated as the number of days it took for a pollutant's concentration to climb back up to or exceed its pre-rainfall level. This metric provides a practical measure of the duration of improved air quality following a precipitation event, indicating how quickly local emissions and atmospheric conditions cause pollution to rebound.

Following the removal of outliers, monthly analyses were conducted for each selected station. The time series of particulate pollutants (PM2.5 and PM10) exhibit clear seasonal patterns, with the highest concentrations during the post-monsoon and winter months (October to February) and lower concentrations during the monsoon season (July to September), a pattern that repeats consistently across the study period. This seasonal cycle is further illustrated in Fig 5. In contrast, ozone (O_3) shows an inverse pattern, with elevated concentrations during the hot, sunny pre- and post-monsoon months, and lower levels during the peak winter pollution episodes. It is also evident that pollutant concentrations are site-specific. Among the selected stations, Anand Vihar consistently shows the highest pollutant levels, particularly for PM10 and NO_x, consistent with previous findings (e.g., Kaushik et al., 2023), which identified Anand Vihar as one of the most polluted regions in Delhi with elevated NO_x concentrations.

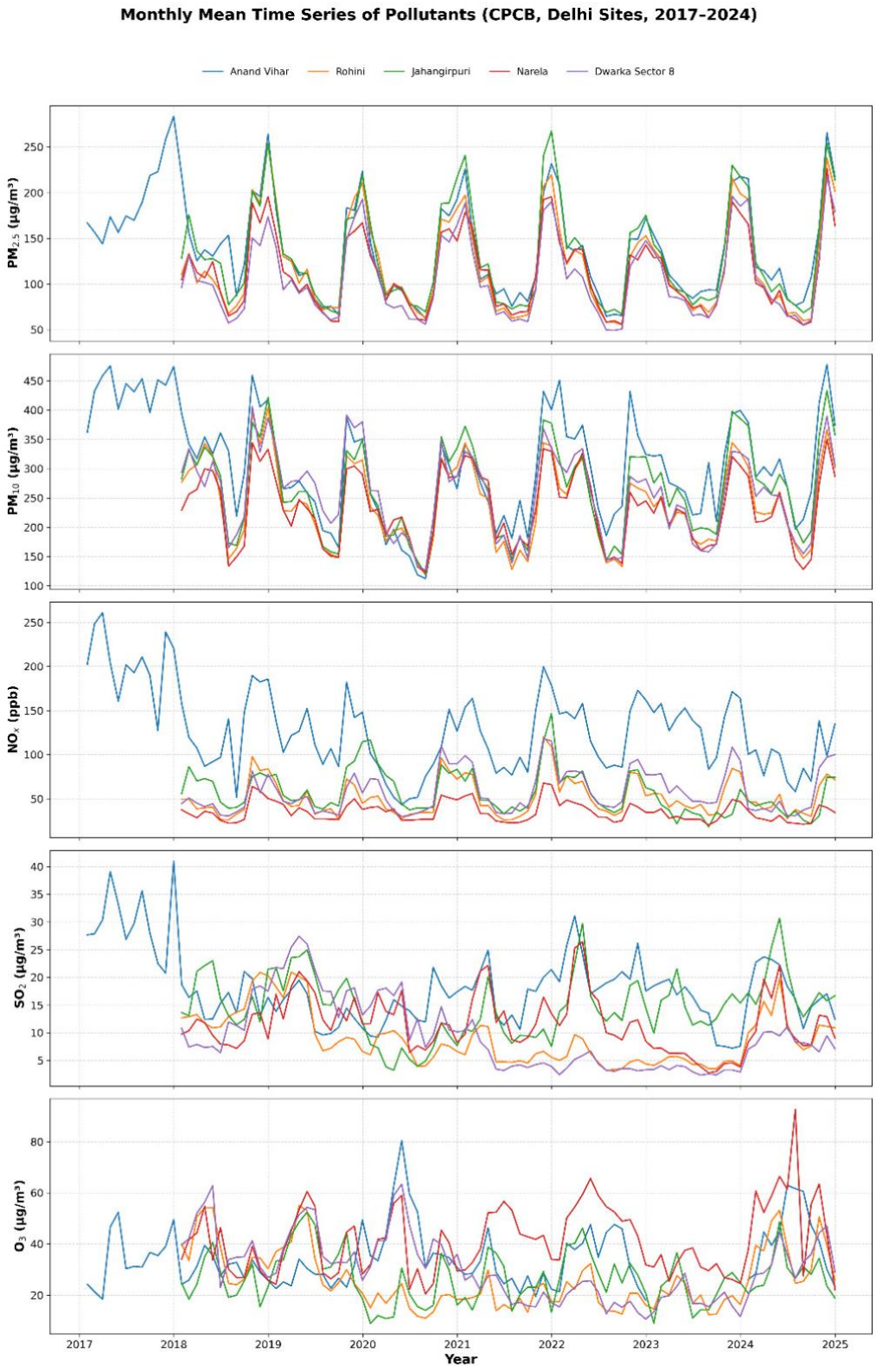

Figure 27: Monthly averaged time series of the criteria pollutants (PM2.5, PM10, NOX, SO_2, O_3) for selected stations (different colours represent different stations) during the period 2017-2024.

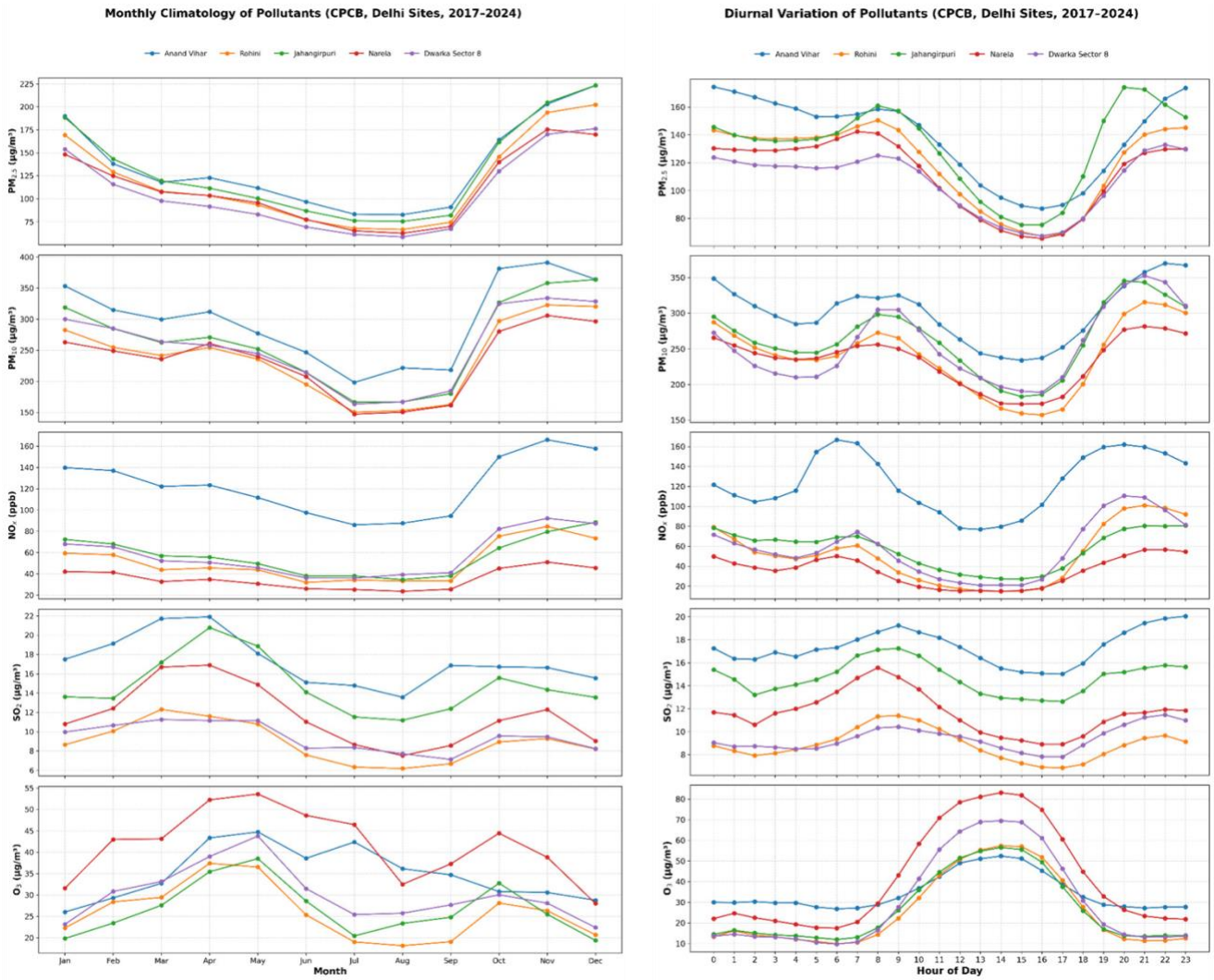

Figure 28: Monthly climatology (left panel) and diurnal variation (right panel) of different criteria air pollutants at the selected stations during the period 2017-2024.

Figure 28 shows the monthly climatology and diurnal variation of different species for selected stations. The seasonal pattern of all the pollutants except ozone shows higher values during the post-monsoon period and lower values during the monsoon in all the stations. However, the ozone shows a different pattern for some stations, like Narela and Anand Vihar (higher values during monsoon). The figure clearly shows that the pollutant levels are specific to the stations, also. Among the selected stations, Anand Vihar shows higher values for all the pollutants except PM2.5. The diurnal variation of most pollutants, excluding ozone, shows a distinct morning peak and afternoon minimum, corresponding to reduced atmospheric mixing in the early morning and enhanced dispersion during the daytime. In contrast, ozone exhibits an opposite pattern, with maximum concentrations in the afternoon due to active photochemical production, and lower concentrations during the early morning hours.

3.2.2. Rainfall classifications

IMD gridded data is available at a daily temporal resolution, whereas the spatial resolution is 0.25-degree for rainfall. The IMD gridded rainfall dataset was prepared by (Pai et al., 2014). Rainfall events were then classified into four categories based on total rainfall intensity according to the IMD report.

- Very light: 0.1 - 2.4 mm
- Light: 2.5 - 7.5 mm
- Moderate: 7.6 - 35.5 mm
- Heavy: > 35.5 mm

Here we considered four types of rainfall events for each station to show how many days experienced very light rain, light rain, moderate rain, and heavy rain (Table 6). Hourly air quality data for key pollutants (PM2.5, PM10, NO_2, and O_3) were obtained from the CPCB network, comprising 81 active continuous monitoring stations across the NCR.In contrast, daily rainfall data for Delhi were collected from the same study period to facilitate correlation with air quality parameters. Specific rainfall episodes were identified according to predefined criteria for intensity (x) and duration (y) thresholds, allowing the isolation of distinct rainfall events for further analysis.

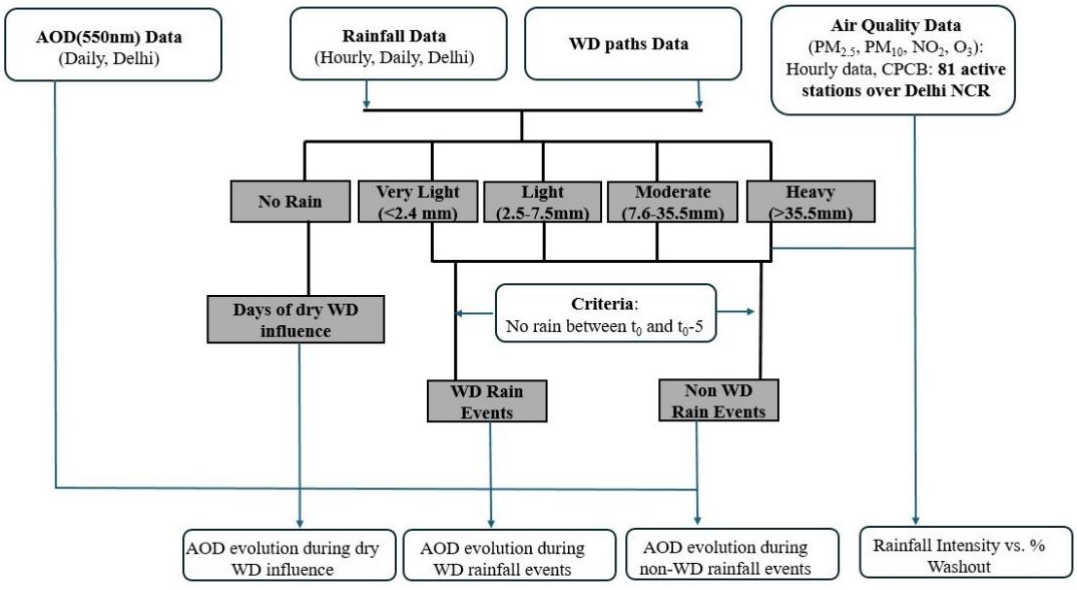

Figure 26: Schematic of the workflow.

We have selected 5 stations with continuous data of both pollutants and wind for further analysis. The analysis has been done for different rainfall events (light, moderate and heavy rainfall events for each station). The details of selected events at the monitoring stations are provided in Table 6.

Table 6: Details of selected rainfall events at the monitoring stations during the period 2019–2024.

STATION	Heavy rain (HR)	Moderate rain (MR)	Light rain (LR)
Anand Vihar	18 Oct 2021	09 Feb 2022	20 Feb 2024
Jahangirpuri	09 Oct 2022	09 Feb 2022	20 Feb 2024
Dwarkar sector-8	18 Oct 2021	01 Feb 2024	20 Feb 2024
Narela	18 Oct 2021	30 Jan 2024	20 Feb 2024
Rohini	18 Oct 2021	9 Feb 2022	20 Feb 2024

3.3 Results

3.3.1. AOD Evolution During Rainfall Events: Western Disturbances vs. Non-WD Events

AOD after WD-rainfall events showed reductions 12.7%, 27.9%, 28.5% for t_0+1, t_0+2, and t_0+3 days respectively when compared to the pre-rain 5 day mean. The AOD reductions of t_0+2 and t_0+3 were statistically significant ($p<0.1$) and others were insignificant for WD-rainfall events (Fig. 30a). The non-WD rainfall events also showed reductions in AOD post rain, but the magnitudes were less for t_0+1 and t_0+2 but higher for t_0+3 when compared to that of WD-rainfall post reductions (Fig. 30b).

The q_{int} curve and AOD curve show similar variation before and after the rainfall events for both WD-rainfall and non-WD rainfall. This can be due to the fact that aerosols absorb moisture and grow in size.

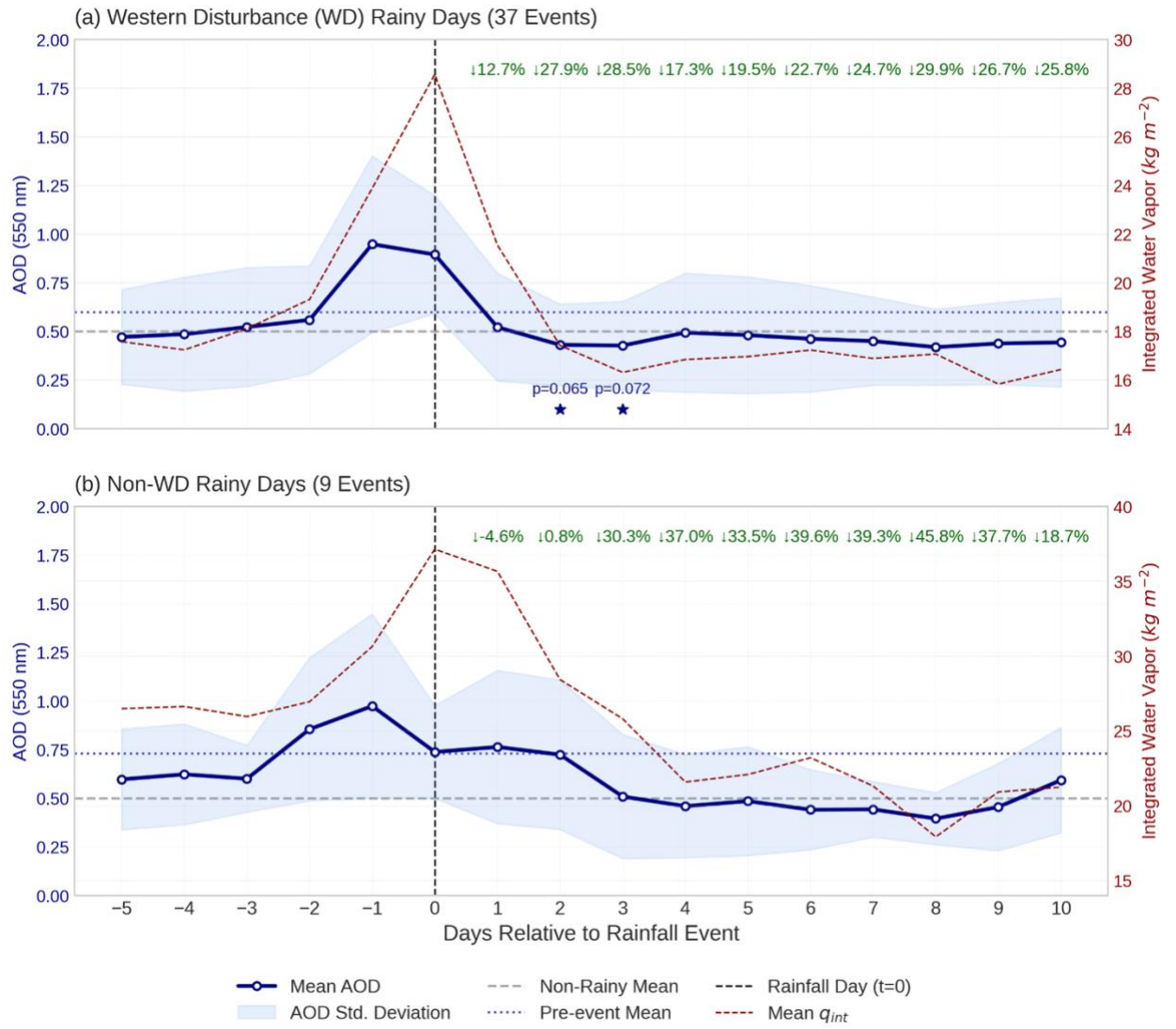

Figure 30: AOD evolution before and after WD-induced and other light and heavy rainfall events.

3.3.2. Rainfall intensity vs washout efficiency

Figure 31 reveals a consistent and clear pattern in Delhi's winter precipitation from 2017 to 2024. Across all five monitoring stations, light rainfall events are by far the most common, occurring frequently throughout the season. Moderate rainfall is significantly less frequent, while heavy, air-cleansing downpours are a rare occurrence, with most sites experiencing only a handful of such events over the entire study period. Interestingly, there is some noticeable geographical variation, as stations like Anand Vihar and Okhla registered more moderate and heavy events compared to Narela, which recorded no heavy events at all. This data suggests that while the city regularly experiences light winter drizzles, the kind of intense rainfall needed for a major pollution washout is an infrequent phenomenon.

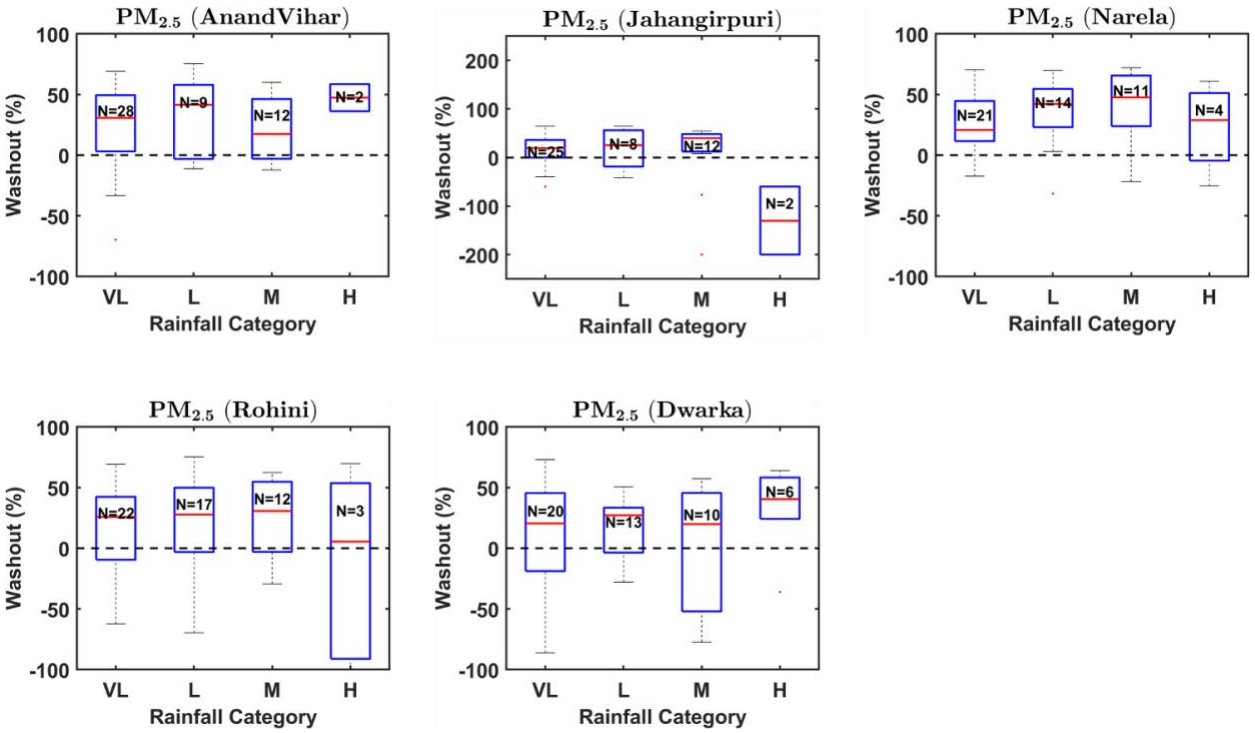

Figure 31: Number of rainfall events at the selected stations during the winter months (October-February) for the period 2017-2024. Rainfall is categorised into [Heavy (H), Moderate (M), Light (L), and Very Light (VL)] rainfall intensities.

This analysis (Figure 32) visualises the relationship between rainfall intensity and its cleansing effect on the atmosphere. For pollutants like particulate matter (PM2.5, PM10) and NOX, there is a clear dose-response pattern: heavy rain is a highly effective scavenger, consistently producing a median washout of 80-95%, while moderate rain's effect is substantial but less potent, and light rain's impact is minimal and highly variable. A striking contrast is seen with ozone, which consistently shows a negative washout-meaning its concentration typically increases after a rain event, likely due to complex photochemical reactions. This highlights that while rainfall is a potent natural cleanser for most primary pollutants, its interaction with secondary pollutants like ozone is far more complex.

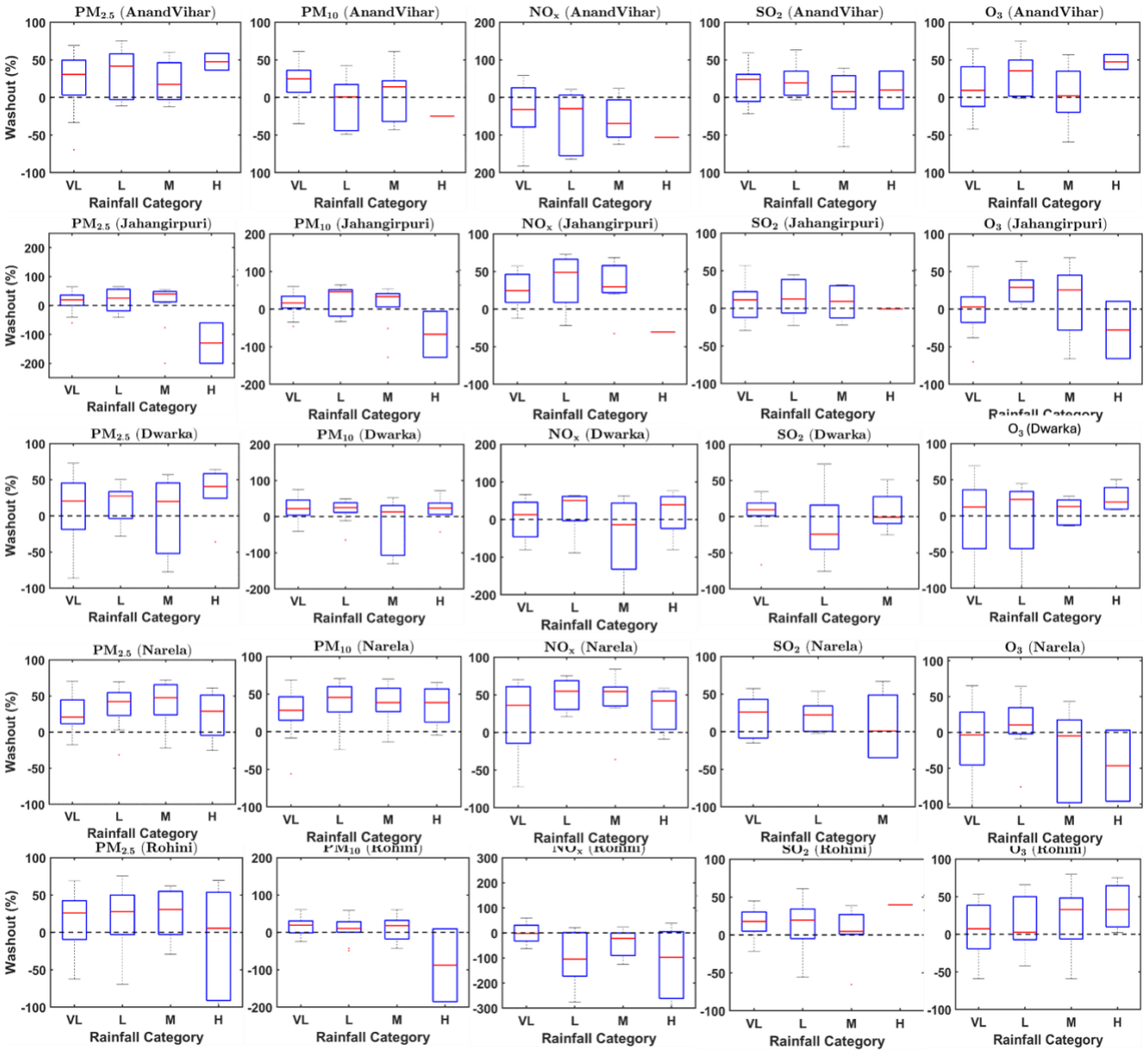

Figure 32: Distribution of pollutant washout percentages following winter rainfall events from 2017 to 2024. The data is grouped by rainfall intensity [Heavy (H), Moderate (M), Light (L), and Very Light (VL)] for five key air pollutants across five Delhi monitoring stations.

3.3.3. AOD Evolution During Dry WD Events

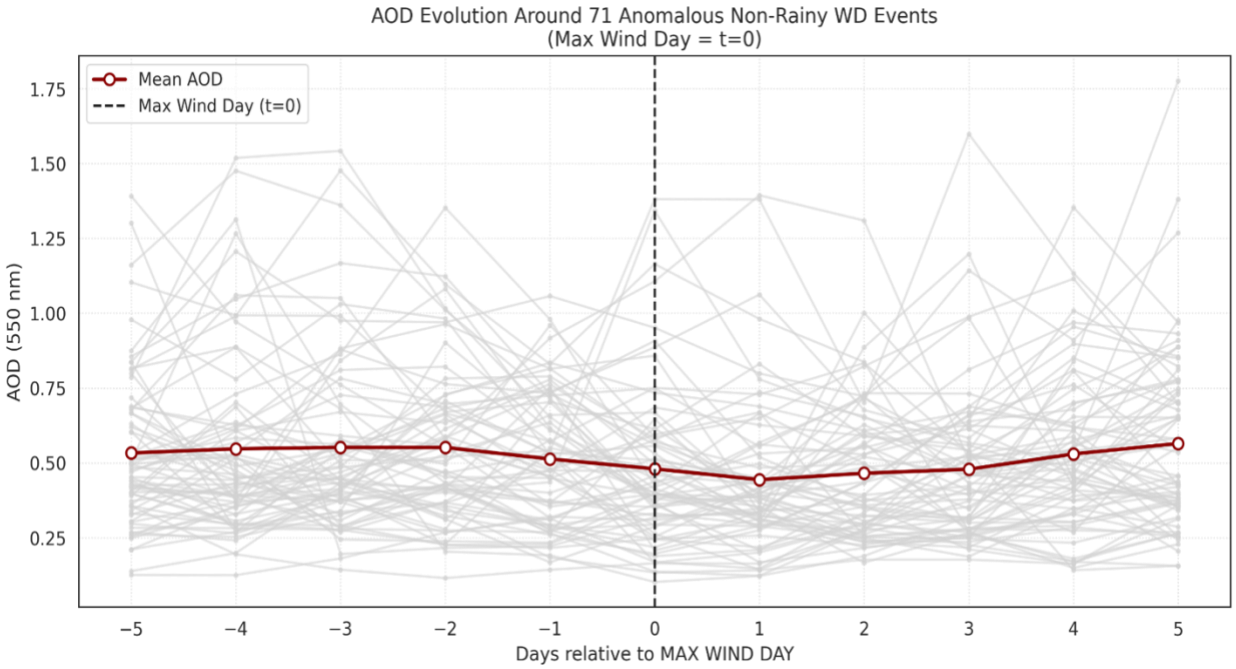

Figure 33: AOD evolution before and after WD-induced and other light and heavy rainfall events

The passage of dry Western Disturbances was associated with a reduction in AOD from day t_0-2 to t_0+1 (Figure 33). However, this reduction was not statistically significant ($p > 0.1$) when compared to the mean AOD on non-rainy days. This decrease in aerosol loading is likely attributable to the synoptic-scale ventilation characteristic of dry WDs, which import cleaner air masses and enhance vertical mixing through increased wind speeds.

3.3.4. Recharge time for pollutants: Case studies

In order to assess the recharge time of each pollutant to regain its original concentration, light, moderate, and heavy rainfall events were analysed at each station. The analysis for Anand Vihar (Figure 34) station clearly demonstrates that the intensity of rainfall has a direct and significant impact on air pollutant concentrations. The heavy rainfall event resulted in a dramatic washout effect, slashing particulate matter levels by over 80% and substantially reducing NOX. This cleaning effect was less pronounced during the moderate rain and was minimal following the light rain, where the dip in pollution was barely distinguishable from daily fluctuations. Interestingly, ozone levels consistently rose immediately after rainfall, highlighting a different atmospheric reaction compared to the other pollutants. While pollution levels begin to rebound in the days following a significant rain event, the recovery to pre-rainfall concentrations is a gradual process, often taking longer than the five-day period observed.

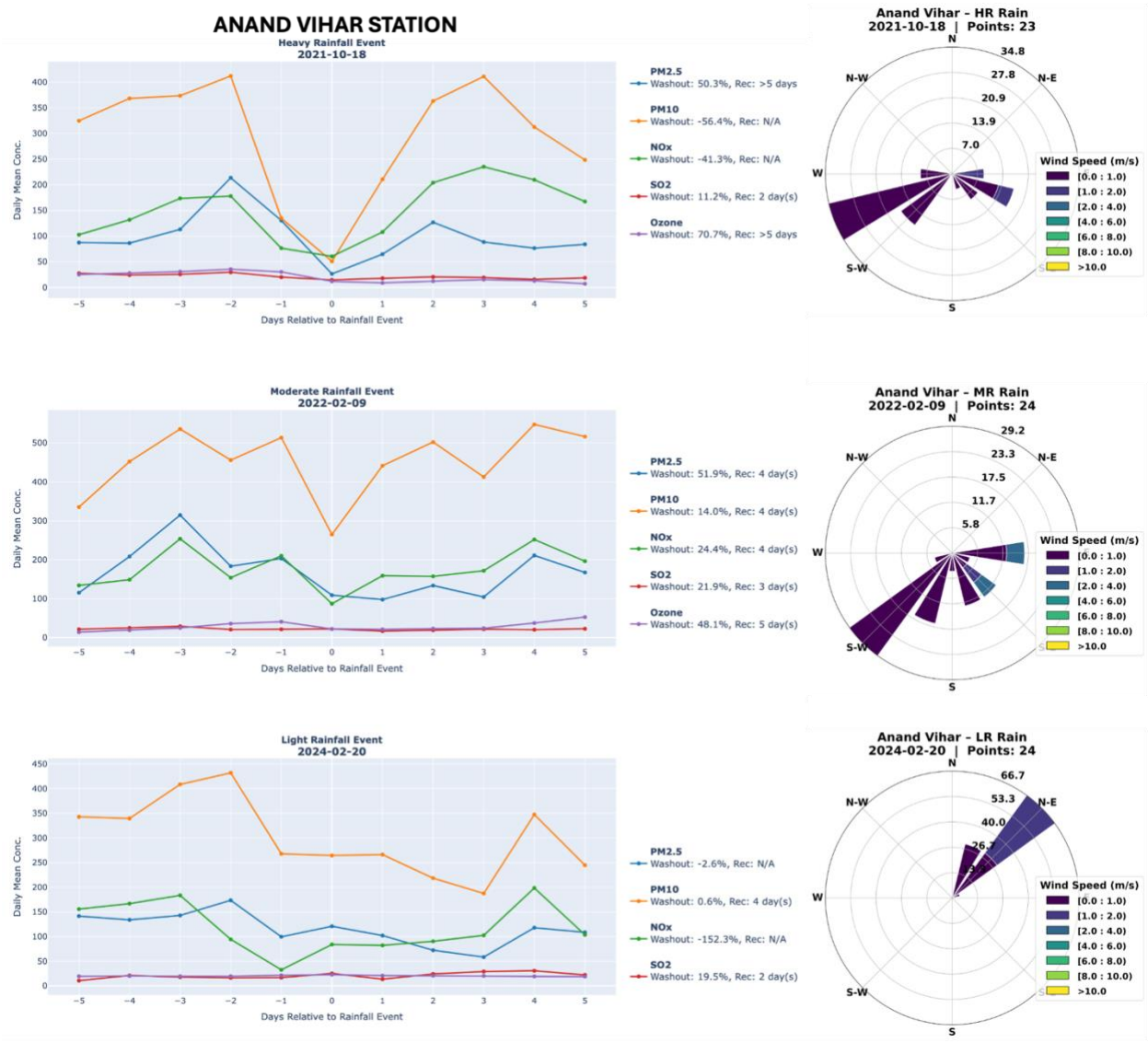

Figure 34: Concentrations of criteria air pollutants at the Anand Vihar station during heavy (upper panel), moderate (middle panel), and light (lower panel) rainfall events, with days relative to rainfall on the x-axis and pollutant concentrations on the y-axis. Each panel includes a corresponding wind rose diagram.

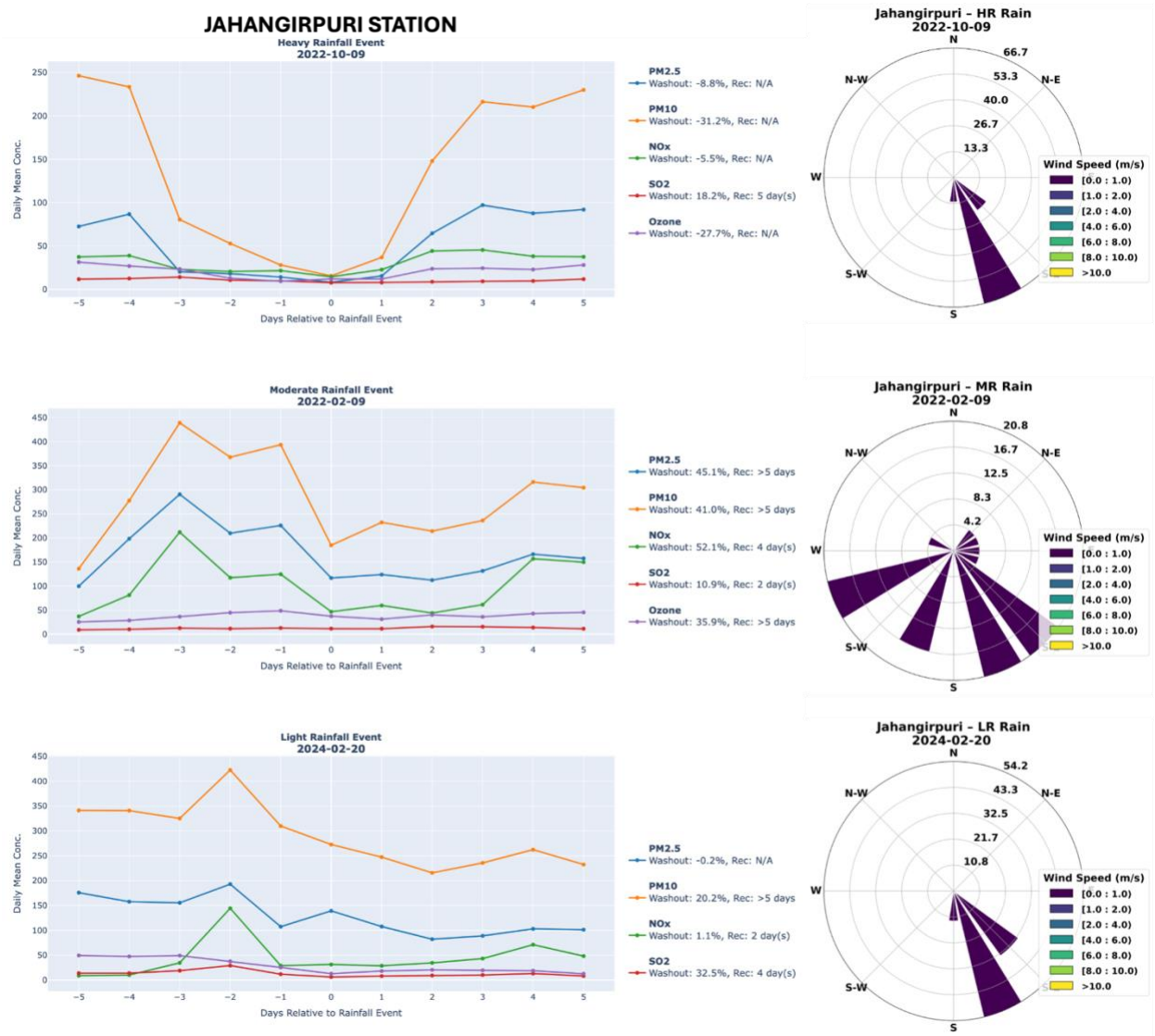

Figure 35: Concentrations of criteria air pollutants at the Jahangirpur station during heavy (upper panel), moderate (middle panel), and light (lower panel) rainfall events, with days relative to rainfall on the x-axis and pollutant concentrations on the y-axis. Each panel includes a corresponding wind rose diagram.

At the Jahangirpuri station (Figure 35), the data illustrate a clear dose-response relationship between rainfall intensity and its cleansing effect on the air. The heavy rainfall event triggered a profound washout, causing particulate matter and NOX concentrations to plummet by over 80-90%. This effect was substantially diminished during the moderate rain, which produced a noticeable but far less dramatic reduction in pollutants. The impact of the light rainfall was marginal, with only a slight dip in pollution that was quickly reversed in the following days. In contrast to other pollutants, ozone consistently exhibited an inverse relationship, increasing in concentration after each rain event, particularly after the heavy downpour. The recovery of particulate and NOX pollution following the most significant washout was slow, indicating that a

single heavy rainfall event can effectively reset air quality for several days before levels begin to creep back up.

Data from Dwarka (Figure 36) shows a clear link between rainfall intensity and its air-cleaning power. The heavy downpour was extremely effective, slashing particulate and NOX pollution by over 90%. While moderate rain also had a significant clearing effect, the light rain barely made a difference. Following a major washout, pollution levels begin a gradual but steady climb back toward their previous concentrations over several days.

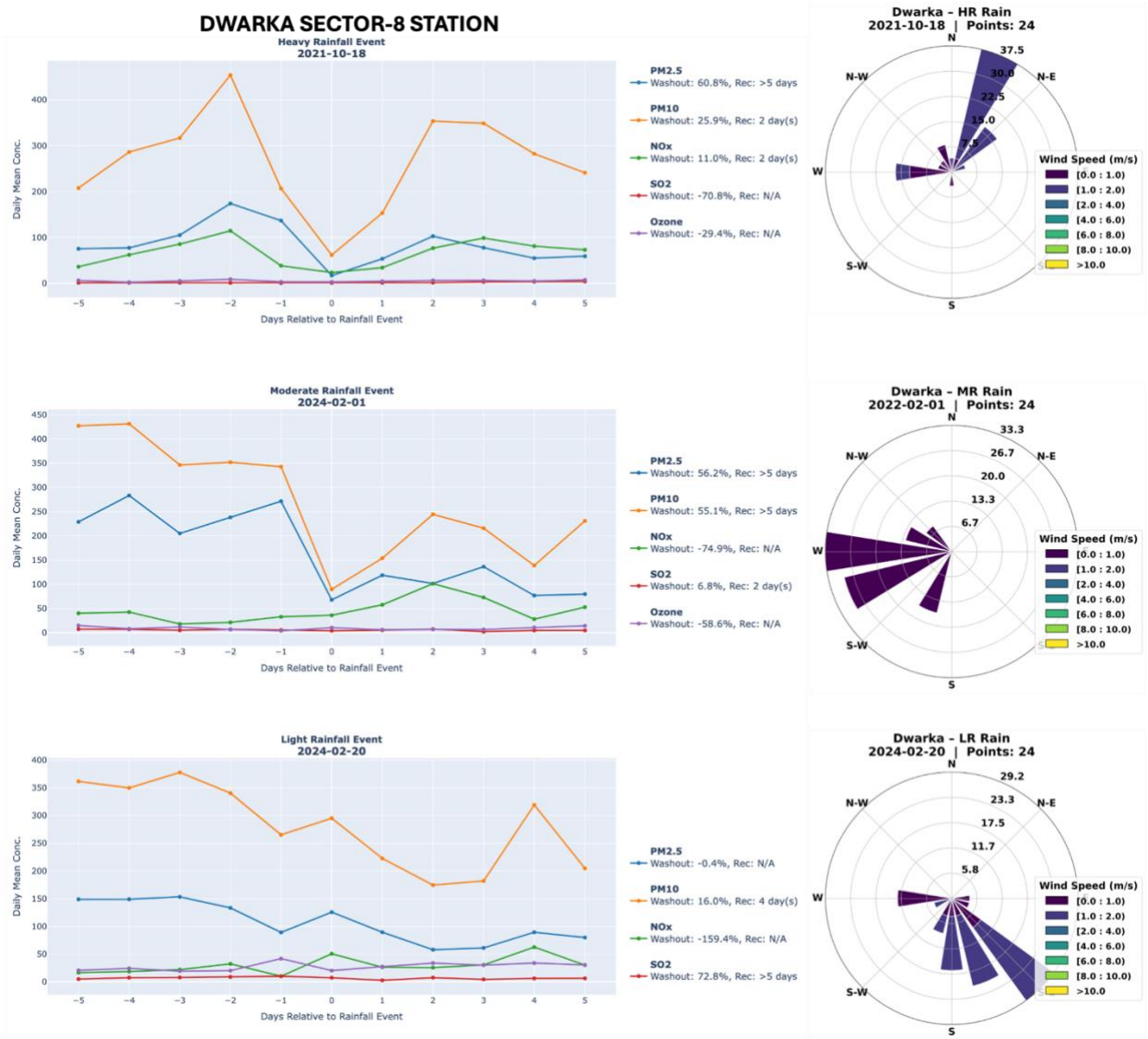

Figure 36: Concentrations of criteria air pollutants at the Dwaraka sector-8 station during heavy (upper panel), moderate (middle panel), and light (lower panel) rainfall events, with days relative to rainfall on the x-axis and pollutant concentrations on the y-axis. Each panel includes a corresponding wind rose diagram.

At the Narela station (Figure 37), the analysis reveals a clear dependence of air pollutant removal efficiency on rainfall intensity. Heavy rainfall events effectively reset the air quality, reducing concentrations of key pollutants such as particulate matter and NOX by more than 95%. Moderate

rainfall also contributes to pollutant removal, though with a markedly lower efficiency compared to heavy rain. In contrast, light rainfall exhibits only a transient and limited cleansing effect, with pollutant concentrations rapidly returning to their pre-event levels. The influence of wind is evident during the moderate rainfall case, where the recharge time for pollutants extends beyond five days, indicating the combined effect of rainfall and other meteorological parameters on post-rain pollution recovery.

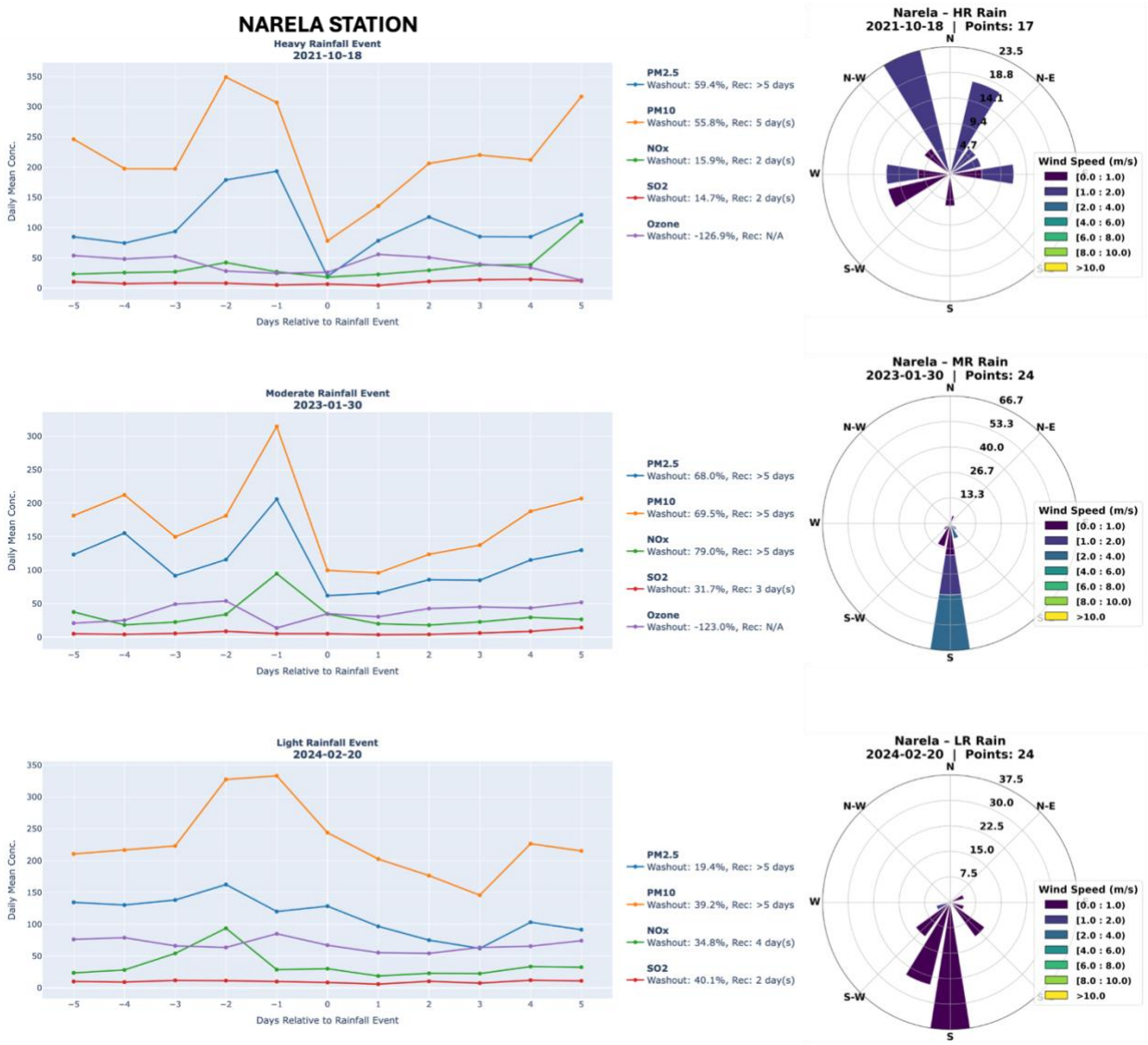

Figure 37: Concentrations of criteria air pollutants at the Narela station during heavy (upper panel), moderate (middle panel), and light (lower panel) rainfall events, with days relative to rainfall on the x-axis and pollutant concentrations on the y-axis. Each panel includes a corresponding wind rose diagram.

The analysis at Rohini station (Figure 38) demonstrates a clear and direct relationship between rainfall intensity and its air-purifying capability. The heavy rainfall event had a profound washout effect, causing a near-total collapse in particulate matter and NOX concentrations with reductions exceeding 90%. This dramatic cleansing was also seen during the moderate rain, which, while less

potent, still managed to slash key pollutant levels by roughly 80%, proving highly effective. In stark contrast, the light rainfall provided only a modest and short-lived dip in pollution, with concentrations quickly rebounding within a day or two. A consistent outlier across all events was ozone, which tended to increase after a downpour, suggesting it is governed by different atmospheric chemistry. Overall, the analysis shows that significant rainfall can effectively reset local air quality for several days, whereas light rain offers only a brief and temporary respite.

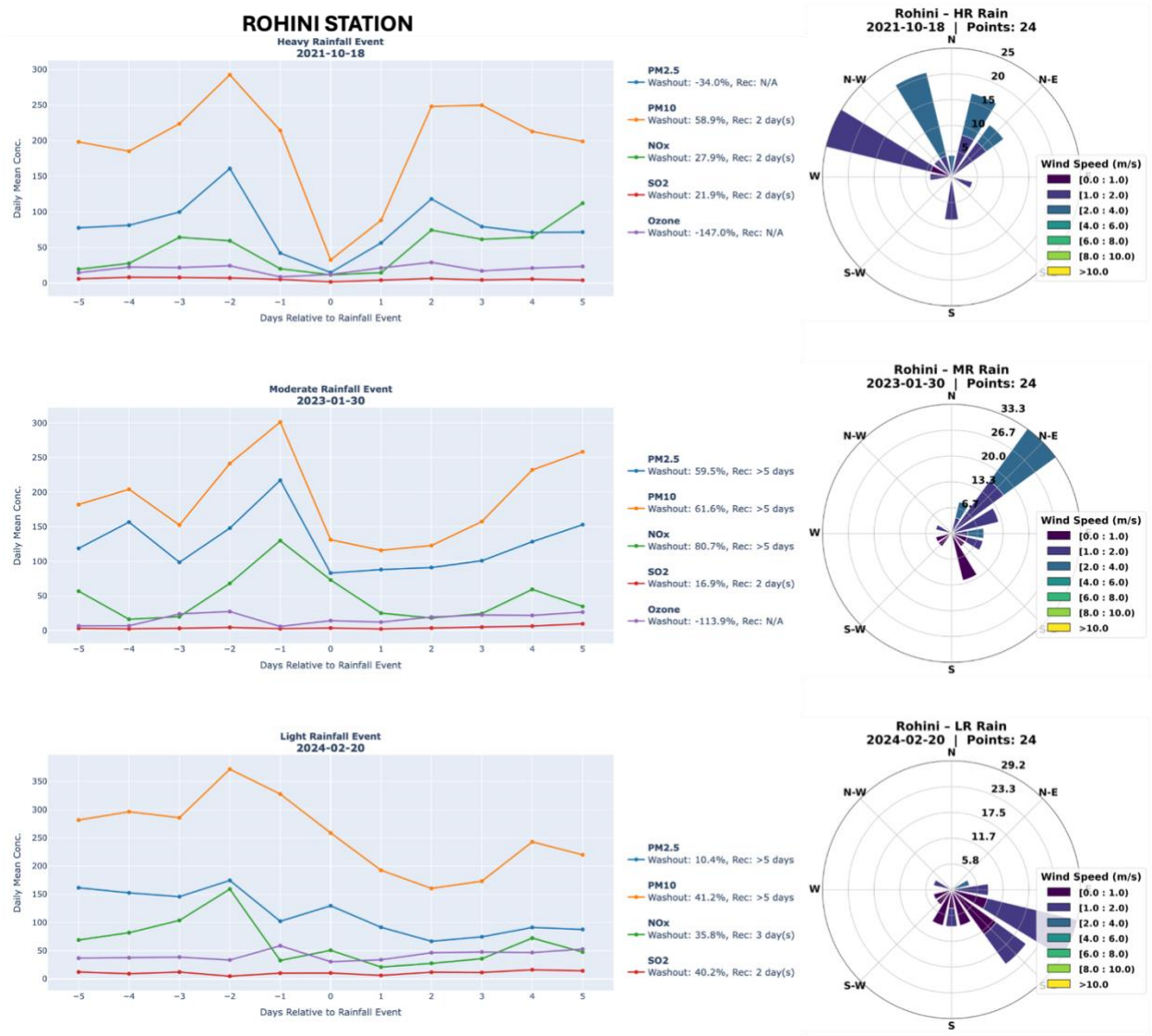

Figure 38: Concentrations of criteria air pollutants at the Rohini station during heavy (upper panel), moderate (middle panel), and light (lower panel) rainfall events, with days relative to rainfall on the x-axis and pollutant concentrations on the y-axis. Each panel includes a corresponding wind rose diagram.

4. Summary and Conclusions

- **Climatological Suitability is Low:** ***Delhi's winter atmosphere is climatologically unsuitable for consistent cloud seeding due to a fundamental lack of sufficient moisture and saturation, particularly during the peak pollution months of December and January.*** A decadal analysis (2011-2021) indicates that the core winter months - December and January-coincide with both the most severe pollution episodes and the driest climatological conditions. Mean TCWV falls below 9 mm, while relative humidity at 850hPa remains between 40-55%, well below the ~80% threshold typically required for sustained cloud formation and persistence.
- **Seedable Days are Quantitatively Rare - Limited Seeding Opportunities:** ***Viable "windows of opportunity" are rare and confined to anomalous weather events, primarily specific types of Western Disturbances. Even days with promising cloud cover and WD presence often lack the necessary combination of moisture depth, saturation, and atmospheric lift, resulting in low MSI scores.*** Application of the MSI provides a quantitative basis for assessing potential cloud seeding opportunities. Days meeting multiple criteria-adequate cloud cover, saturation, lift, liquid water content, and suitable freezing levels-are infrequent. The most promising subset, classified as *Western Disturbance days without rainfall*, averages only about one to two days per month. This finding confirms that thermodynamic conditions conducive to seeding are anomalous rather than typical.
- **Identified Potential Days:** ***Despite the overall poor conditions, analysis identified 92 days over the decade with moisture and cloud cover comparable to naturally occurring moderate-to-heavy rainfall days (>7.5 mm), representing the upper limit of potential opportunities.***
- **Synoptic Control is Dominant:** ***The analysis identifies Western Disturbances as the primary synoptic-scale mechanism capable of generating potential seeding conditions. However, the majority of WD-influenced days are either dry or produce only light precipitation, failing to provide the necessary confluence of moisture and dynamic lift required for confident seeding operations.***
- **Aerosol Vertical Structure Poses Targeting Challenges:** ***Observations from CALIPSO and ground-based ceilometers show that aerosol concentrations are predominantly confined to a shallow boundary layer below 2 km, whereas seedable cloud layers during winter are typically located between 2-5 km. This vertical separation complicates the***

delivery and activation of seeding agents, reducing the likelihood of effective aerosol - cloud interaction.

- **Aerosol-Cloud Interactions:** ***High aerosol concentrations during winter are associated with increased cloud cover, lower cloud base heights (CBH < 2-4 km), and higher cloud liquid/ice water content, particularly during rainy conditions (both WD-associated and non-WD associated).*** This suggests aerosols significantly influence cloud microphysics and potentially favor ice nucleation processes at high AOD levels.
- **Cloud Microphysics are Linked to Pre-existing Rainfall:** ***Analysis of cloud properties across AOD bins reveals that favorable microphysical conditions for seeding- specifically, low cloud bases (<4 km, suitable for aircraft access) and high liquid or ice water content - tend to occur on days already experiencing natural precipitation.*** This limits the potential marginal benefit of seeding, as enhancing rainfall from already precipitating clouds offers uncertain efficacy.
- **Pollution Alters the Baseline Cloud Regime:** A positive correlation between high AOD and both lower cloud bases and higher water content suggests that Delhi's polluted atmosphere, rich in CCN, modifies cloud microphysics. ***While seeding could theoretically counteract precipitation suppression caused by numerous small droplets, the nonlinear and complex aerosol-cloud interactions in such an environment make outcomes highly unpredictable.***
- **Seeding Methodology:** ***The thermal structure indicates glaciogenic seeding (e.g., using AgI) is potentially viable during core winter (Dec-Jan) when temperatures at cloud level are below freezing, while hygroscopic seeding is less promising during this period.***
- **Operational Feasibility:** ***Aircraft-based seeding (typically around 2km altitude) appears operationally feasible primarily during rainy conditions (WDR and NWDR) when CBH is sufficiently low, coinciding with medium-to-high AOD levels.***
- **Washout Efficiency is Strongly Dose-Dependent:** Rainfall intensity exhibits a clear nonlinear relationship with pollutant scavenging. ***Heavy rainfall (>35.5 mm) achieves substantial reductions in $PM_{2.5}$, PM_{10}, and NO_x concentrations (>80-95%), while light rainfall (<7.5 mm) provides only limited and variable washout (<30%), often within the range of statistical uncertainty.***
- **Air Quality Improvements/Pollutant Recovery are Short-Lived:** ***Analysis of "recharge time" across five monitoring stations shows that even after heavy rainfall-or a hypothetically successful seeding event-pollutant concentrations typically return to pre-event levels within 1-5 days.*** Persistent emissions and the re-establishment of stable

boundary-layer conditions drive this rapid rebound, sharply limiting the duration of any improvement. Following rainfall events, pollutant levels typically recover within 4-5 days for PM2.5/PM10 and 2-3 days for NOX/SO_2, though recovery times are strongly influenced by prevailing meteorological conditions like wind speed.

- **Ozone Dynamics Respond Adversely:** ***A consistent finding is that rainfall events often coincide with negative washout effects for ozone, with concentrations tending to rise post-event.*** This pattern indicates that cloud seeding is ineffective for ozone mitigation and may temporarily exacerbate this pollutant.
- **Ventilation by Dry Western Disturbances Provides Limited Relief:** ***Dry WDs can reduce AOD by approximately 10-20% through enhanced wind speeds and vertical mixing, offering a secondary mechanism for pollutant dispersion.*** However, this effect is weaker and less consistent than wet scavenging.
- **Major Concerns & Limitations:** ***Significant concerns remain regarding the environmental and health impacts of seeding agents like AgI (toxicity, bioaccumulation), the high operational costs, and the uncertainty of large-scale effectiveness. Cloud seeding should be viewed as a potential emergency, short-term measure rather than a sustainable long-term solution, which requires integrated emission control strategies.***

While cloud seeding is theoretically feasible under specific atmospheric conditions, during Delhi's winter, its practical utility as a consistent and reliable air-quality intervention is constrained. The necessary atmospheric conditions are rare and frequently coincide with natural rainfall, limiting the potential marginal gain. Even when successful, induced rainfall would likely provide only a brief respite (typically one to three days) before pollution levels rebound. Given the high operational costs, the scientific uncertainties inherent in aerosol-laden environments, and the absence of any impact on underlying emission sources, cloud seeding cannot be recommended as a primary or strategic measure for Delhi's pollution management. At best, it could serve as a high-cost, tactical intervention during declared air-quality emergencies, contingent upon a forecast meeting stringent MSI-based suitability criteria. Ultimately, the study underscores that sustained emission reduction remains the best viable and durable solution to Delhi's chronic air pollution crisis.

References

1. Arun, S. H., Sharma, S. K., Chaurasia, S., Vaishnav, R., & Kumar, R. (2018). Fog/low clouds detection over the Delhi Earth Station using the Ceilometer and the INSAT-3D/3DR satellite data. *International Journal of Remote Sensing*, 39(12), 4130–4144. https://doi.org/10.1080/01431161.2018.1454624
2. Azeez, H. M., Ibraheem, N. T., & Hussain, H. H. (2024). Alternate Chemical Compounds as a Condensation Nucleus in Cloud Seeding. *Nature Environment and Pollution Technology*, *23*(3), 1795–1799. https://doi.org/10.46488/NEPT.2024.V23I03.052
3. Breed, D., Rasmussen, R., Weeks, C., Boe, B., & Deshler, T. (2014). Evaluating Winter Orographic Cloud Seeding: Design of the Wyoming Weather Modification Pilot Project (WWMPP). *Journal of Applied Meteorology and Climatology*, *53*(2), 282–299. https://doi.org/10.1175/JAMC-D-13-0128.1
4. Bruintjes, R. T. (1999). A review of cloud seeding experiments to enhance precipitation. *Bulletin of the American Meteorological Society*, 80(5), 805-820
5. *CAIPEEX Cloud Physics Literacy Course Report* (2023). Indian Institute of Tropical Meteorology. Retrieved from https://www.tropmet.res.in/~lip/Publication/Technical-Reports/CAIPEEX-Report-July2023.pdf
6. Chen, M., Jing, X., Li, J., Yang, J., Dong, X., Geerts, B., Yin, Y., Chen, B., Xue, L., Huang, M., Tian, P., & Hua, S. (2025). Accelerated impact of airborne glaciogenic seeding of stratiform clouds by turbulence. *Atmospheric Chemistry and Physics*, *25*(14), 7581–7596. https://doi.org/10.5194/ACP-25-7581-2025
7. Chen, S., Xue, L., Tessendorf, S. A., Chubb, T., Peace, A., Kenyon, S., Speirs, J., Wolff, J., & Petzke, B. (2025). Assessing glaciogenic seeding impacts in Australia's Snowy Mountains: an ensemble modeling approach. *Atmospheric Chemistry and Physics*, *25*(13), 6703–6724. https://doi.org/10.5194/ACP-25-6703-2025
8. Chowdhury, S., Dey, S., Ghosh, S. et al. Satellite-Based Estimates of Aerosol Washout and Recovery over India during Monsoon. Aerosol Air Qual. Res. 16, 1302–1314 (2016). https://doi.org/10.4209/aaqr.2015.01.0018
9. Fajardo, C., Costa, G., Ortiz, L., Nande, M., Rodríguez-Membibre, M., Martín, M., & Sánchez-Fortún, S. (2016). Potential risk of acute toxicity induced by AgI cloud seeding on soil and freshwater biota. *Ecotoxicology and Environmental Safety*, *133*, 433–441. https://doi.org/10.1016/j.ecoenv.2016.06.028
10. Farahat, A., & Abuelgasim, A. (2022). Effect of cloud seeding on aerosol properties and particulate matter variability in the United Arab Emirates. *International Journal of Environmental Science and Technology*, *19*(2), 951–968. https://doi.org/10.1007/S13762-020-03057-5/FIGURES/11
11. Forest Survey of India. *State of Forest Report*; Ministry of Environment & Forests: Dehradun, India, 2011.
12. Freud, E., Koussevitzky, H., Goren, T., & Rosenfeld, D. (2015). Cloud microphysical background for the Israel-4 cloud seeding experiment. *Atmospheric Research*, *158–159*, 122–138. https://doi.org/10.1016/J.ATMOSRES.2015.02.007

13. Fujino, R., Miyamoto, Y., & Kiryu, T. (2025). PM2. 5 concentration decreases with snowfall as revealed by surface observation data. *SOLA*, *21*, 101-107, https://doi.org/10.2151/sola.2025-013.
14. Gani, S., Bhandari, S., Seraj, S., Wang, D. S., Patel, K., Soni, P., Arub, Z., Habib, G., Hildebrandt Ruiz, L., and Apte, J. S.: Submicron aerosol composition in the world's most polluted megacity: the Delhi Aerosol Supersite study, Atmos. Chem. Phys., 19, 6843–6859, https://doi.org/10.5194/acp-19-6843-2019
15. Gautam, A. S., Tripathi, S. N., Joshi, A., Mandariya, A. K., Singh, K., Mishra, G., Kumar, S., & Ramola, R. C. (2021a). First surface measurement of variation of Cloud Condensation Nuclei (CCN) concentration over the Pristine Himalayan region of Garhwal, Uttarakhand, India. *Atmospheric Environment*, *246*, 118123. https://doi.org/10.1016/J.ATMOSENV.2020.118123
16. Gautam, A. S., Tripathi, S. N., Joshi, A., Mandariya, A. K., Singh, K., Mishra, G., Kumar, S., & Ramola, R. C. (2021b). First surface measurement of variation of Cloud Condensation Nuclei (CCN) concentration over the Pristine Himalayan region of Garhwal, Uttarakhand, India. *Atmospheric Environment*, *246*, 118123. https://doi.org/10.1016/J.ATMOSENV.2020.118123
17. Geerts, B., & Rauber, R. M. (2022). Glaciogenic Seeding of Cold-Season Orographic Clouds to Enhance Precipitation: Status and Prospects. *Bulletin of the American Meteorological Society*, *103*(10), E2302–E2314. https://doi.org/10.1175/BAMS-D-21-0279.1
18. Givati, Amir, and Daniel Rosenfeld. "Separation between cloud-seeding and air-pollution effects." Journal of Applied Meteorology 44.9 (2005): 1298-1314.
19. Global Modeling and Assimilation Office (GMAO) (2015), inst3_3d_asm_Cp: MERRA-2 3D IAU State, Meteorology Instantaneous 3-hourly (p-coord, 0.625x0.5L42), version 5.12.4, Greenbelt, MD, USA: Goddard Space Flight Center Distributed Active Archive Center (GSFC DAAC), Accessed Enter User Data Access Date at doi: 10.5067/VJAFPLI1CSIV.
20. Guo, X., & Zheng, G. (2009). Advances in weather modification from 1997 to 2007 in China. *Advances in Atmospheric Sciences*, *26*(2), 240–252. https://doi.org/10.1007/S00376-009-0240-8/METRICS
21. Guttikunda, S. K., & Calori, G. (2013). A GIS based emissions inventory at 1 km× 1 km spatial resolution for air pollution analysis in Delhi, India. *Atmospheric Environment*, *67*, 101-111. https://doi.org/10.1016/j.atmosenv.2012.10.040
22. Hegg, D. A., Clarke, A. D., Doherty, S. J., & Ström4, J. (2011). Measurements of black carbon aerosol washout ratio on Svalbard. *Tellus B: Chemical and Physical Meteorology*, *63*(5), 891-900, https://doi.org/10.1111/j.1600-0889.2011.00577.x
23. Hersbach H, Bell B, Berrisford P, et al. The ERA5 global reanalysis. Q J R Meteorol Soc. 2020; 146: 1999–2049. https://doi.org/10.1002/qj.3803
24. Hunt, K. M. R., Baudouin, J., Turner, A. G., Dimri, A. P., Jeelani, G., Chattopadhyay, R., Cannon, F., Arulalan, T., Shekhar, M. S., Sabin, T. P., & Palazzi, E. (2025). Western disturbances and climate variability: a review of recent developments. Weather and Climate Dynamics, 6(1), 43–112. https://doi.org/10.5194/wcd-6-43-2025

25. Hunt, K. M. R., Turner, A. G., & Shaffrey, L. C. (2019). Falling trend of Western disturbances in future climate simulations. *Journal of Climate*, *32*(16), 5037–5051. https://doi.org/10.1175/jcli-d-18-0601.1
26. Hunt, K.M.R., Turner, A.G. and Shaffrey, L.C. (2018), The evolution, seasonality and impacts of western disturbances. Q.J.R. Meteorol. Soc., 144: 278-290. https://doi.org/10.1002/qj.3200
27. Jones, A. C., Hill, A., Hemmings, J., Lemaitre, P., Quérel, A., Ryder, C. L., and Woodward, S.: Below-cloud scavenging of aerosol by rain: a review of numerical modelling approaches and sensitivity simulations with mineral dust in the Met Office's Unified Model, Atmos. Chem. Phys., 22, 11381–11407, https://doi.org/10.5194/acp-22-11381-2022
28. Kalsi, S. R. and Halder, S. R.: Satellite observations of interaction between tropics and mid-latitudes, Mausam, 43, 59–64, 1992. https://wcd.copernicus.org/articles/6/43/2025/#xref_paren.184, https://wcd.copernicus.org/articles/6/43/2025/#xref_text.186, https://wcd.copernicus.org/articles/6/43/2025/#xref_text.188
29. Kaushik, N., & Das, R. M. (2023). Investigation of NOX and related secondary pollutants at Anand Vihar, one of the most polluted area of Delhi. *Urban Climate*, *52*, 101747.
30. Koren, I., Feingold, G., & Remer, L. A. (2010). The invigoration of deep convective clouds over the Atlantic: Aerosol effect, meteorology or retrieval artifact? *Atmospheric Chemistry and Physics*, *10*(18), 8855–8872. https://doi.org/10.5194/ACP-10-8855-2010
31. Ku, J. M., Chang, K. H., Chae, S., Ko, A. R., Ro, Y., Jung, W., & Lee, C. (2023a). Preliminary Results of Cloud Seeding Experiments for Air Pollution Reduction in 2020. *Asia-Pacific Journal of Atmospheric Sciences*, *59*(3), 347–358. https://doi.org/10.1007/S13143-023-00315-7/FIGURES/9
32. Ku, J. M., Chang, K. H., Chae, S., Ko, A. R., Ro, Y., Jung, W., & Lee, C. (2023b). Preliminary Results of Cloud Seeding Experiments for Air Pollution Reduction in 2020. *Asia-Pacific Journal of Atmospheric Sciences*, *59*(3), 347–358. https://doi.org/10.1007/S13143-023-00315-7/FIGURES/9
33. Ku, Jung Mo, et al. "Preliminary results of cloud seeding experiments for air pollution reduction in 2020." Asia-Pacific Journal of Atmospheric Sciences 59.3 (2023): 347-358.
34. Kulkarni, J. R., Morwal, S. B., & Deshpande, N. R. (2019). Rainfall enhancement in Karnataka state cloud seeding program "Varshadhare" 2017. *Atmospheric Research*, *219*, 65–76. https://doi.org/10.1016/J.ATMOSRES.2018.12.020
35. Kumar, Mohit and Chakravarty, Kaustav and Deshpande, Sachin and Mise, Dhwanit J., Analyzing the Atmospheric Dynamics, Thermodynamics and Cloud Microphysics in Two Rainfall Events Over the Delhi Region. Available at SSRN: https://ssrn.com/abstract=5215126 or http://dx.doi.org/10.2139/ssrn.5215126
36. Lu, X., Chan, S. C., Fung, J. C., & Lau, A. K. (2019). To what extent can the below-cloud washout effect influence the PM2. 5? A combined observational and modeling study. *Environmental Pollution*, *251*, 338-343, https://doi.org/10.1016/j.envpol.2019.04.06
37. Luan, T., Guo, X., Zhang, T. et al. Below-Cloud Aerosol Scavenging by Different-Intensity Rains in Beijing City. J Meteorol Res 33, 126–137 (2019). https://doi.org/10.1007/s13351-019-8079-0

38. Malik, Shaista, et al. "Cloud seeding; its prospects and concerns in the modern world-A review." Int. J. Pure App. Biosci 6.5 (2018): 791-796.
39. Maria, S. F., & Russell, L. M. (2005). Organic and inorganic aerosol below-cloud scavenging by suburban New Jersey precipitation. *Environmental science & technology*, *39*(13), 4793-4800, https://doi.org/10.1021/es0491679
40. Murthy, B., Latha, R., Tiwari, A., Rathod, A., Singh, S., & Beig, G. (2020). Impact of mixing layer height on air quality in winter. *Journal of Atmospheric and Solar-Terrestrial Physics*, 197, 105157. https://doi.org/10.1016/j.jastp.2019.105157
41. Neyman, J., Osborn, H. B., Scott, E. L., & Wells, M. A. (1972). Re-Evaluation of the Arizona Cloud-Seeding Experiment. *Proceedings of the National Academy of Sciences*, *69*(6), 1348–1352. https://doi.org/10.1073/PNAS.69.6.1348
42. Pai D.S., Latha Sridhar, Rajeevan M., Sreejith O.P., Satbhai N.S. and Mukhopadhyay B., 2014: Development of a new high spatial resolution (0.25° X 0.25°) Long period (1901-2010) daily gridded rainfall data set over India and its comparison with existing data sets over the region; MAUSAM, 65, 1(January 2014), pp1-18.
43. Pokharel, B., & Geerts, B. (2016a). A multi-sensor study of the impact of ground-based glaciogenic seeding on clouds and precipitation over mountains in Wyoming. Part I: Project description. *Atmospheric Research*, *182*, 269–281. https://doi.org/10.1016/J.ATMOSRES.2016.08.008
44. Pokharel, B., & Geerts, B. (2016b). A multi-sensor study of the impact of ground-based glaciogenic seeding on clouds and precipitation over mountains in Wyoming. Part I: Project description. *Atmospheric Research*, *182*, 269–281. https://doi.org/10.1016/J.ATMOSRES.2016.08.008
45. Pourghasemi, M. A., Memarian, M. H., & Zare, A. (2022). Assessment of Possible Precipitation Enhancement by Glaciogenic Cloud Seeding Using WRF: A Case Study. *Russian Meteorology and Hydrology*, *47*(7), 553–560. https://doi.org/10.3103/S106837392207010X/FIGURES/3
46. Prabhakaran, T., Murugavel, P., Konwar, M., Malap, N., Gayatri, K., Dixit, S., Samanta, S., Chowdhuri, S., Bera, S., Varghese, M., Rao, J., Sandeep, J., Safai, P. D., Sahai, A. K., Axisa, D., Karipot, A., Baumgardner, D., Werden, B., Fortner, E., … Nanjundiah, R. (2023). CAIPEEX: Indian Cloud Seeding Scientific Experiment. *Bulletin of the American Meteorological Society*, *104*(11), E2095–E2120. https://doi.org/10.1175/BAMS-D-21-0291.1
47. Rosenfeld, D., Yu, X., Liu, G., Xu, X., Zhu, Y., Yue, Z., Dai, J., Dong, Z., Dong, Y., Peng, Y., Yu, X., Liu, G., Xu, X., Zhu, Y., Yue, Z., Dai, J., Dong, Z., Dong, Y., & Peng, Y. (2011a). Glaciation temperatures of convective clouds ingesting desert dust, air pollution and smoke from forest fires. *Geophysical Research Letters*, *38*(21). https://doi.org/10.1029/2011GL049423
48. Rosenfeld, D., Yu, X., Liu, G., Xu, X., Zhu, Y., Yue, Z., Dai, J., Dong, Z., Dong, Y., Peng, Y., Yu, X., Liu, G., Xu, X., Zhu, Y., Yue, Z., Dai, J., Dong, Z., Dong, Y., & Peng, Y. (2011b). Glaciation temperatures of convective clouds ingesting desert dust, air pollution and smoke from forest fires. *Geophysical Research Letters*, *38*(21). https://doi.org/10.1029/2011GL049423

49. Roy, A., Chatterjee, A., Ghosh, A., Das, S. K., Ghosh, S. K., & Raha, S. (2019). Below-cloud scavenging of size-segregated aerosols and its effect on rainwater acidity and nutrient deposition: A long-term (2009–2018) and real-time observation over eastern Himalaya. Science of The Total Environment, 674, 223–233. https://doi.org/10.1016/j.scitotenv.2019.04.165
50. Seinfeld, J. H., & Pandis, S. N. (2016). *Atmospheric chemistry and physics: From air pollution to climate change* (3rd ed.). Wiley.
51. Super, A. B. (1990). Winter Orographic Cloud Seeding Status in the Intermountain West. *The Journal of Weather Modification*, *22*(1), 106–116. https://doi.org/10.54782/JWM.V22I1.342
52. Tan, I., Storelvmo, T., & Choi, Y. S. (2014). Spaceborne lidar observations of the ice-nucleating potential of dust, polluted dust, and smoke aerosols in mixed-phase clouds. *Journal of Geophysical Research: Atmospheres*, *119*(11), 6653–6665. https://doi.org/10.1002/2013JD021333
53. Teller, A., Axisa, D., Breed, D., & Bruintjes, R. J12. 2 THE EFFECTS OF GIANT CCN ON CLOUDS AND PRECIPITATION: A CASE STUDY FROM THE SAUDI ARABIA PROGRAM FOR THE ASSESSMENT OF RAINFALL AUGMENTATION.
54. *The Second Israeli Randomized Cloud Seeding Experiment: Evaluation of the Results in: Journal of Applied Meteorology and Climatology Volume 20 Issue 11 (1981)*. (n.d.). Retrieved October 24, 2025, from https://journals.ametsoc.org/view/journals/apme/20/11/1520-0450_1981_020_1301_tsircs_2_0_co_2.xml
55. Tiwari, S., Beig, G., & Kumar, P. (2015). Black carbon and aerosol chemical composition in urban India. *Atmospheric Pollution Research, 6,* 107–121. https://doi.org/10.5094/APR.2015.013
56. Tripathi, A., Misra, A. K., & Shukla, J. B. (2022). A mathematical model for the removal of pollutants from the atmosphere through artificial rain. *Stochastic Analysis and Applications*, *40*(3), 379–396. https://doi.org/10.1080/07362994.2021.1915802
57. UNDP. (2024). Multi-Sectoral Action Plan for Air Pollution Mitigation in Gurugram,India 2025-2030. United Nations Development Programme. Licence: CC BY-NC-SA 3.0 IGO. https://www.undp.org/sites/g/files/zskgke326/files/2025-02/multi-sectoral_action_plan_for_air_pollution_mitigation_in_gurugram_india_2025-2030.pdf
58. Wehbe, Y., Tessendorf, S. A., Weeks, C., Bruintjes, R., Xue, L., Rasmussen, R., Lawson, P., Woods, S., & Temimi, M. (2021). Analysis of aerosol-cloud interactions and their implications for precipitation formation using aircraft observations over the United Arab Emirates. *Atmospheric Chemistry and Physics*, *21*(16), 12543–12560. https://doi.org/10.5194/ACP-21-12543-2021
59. Woodley, W. (2003). *Results of On-Top Glaciogenic Cloud Seeding in Thailand. Part I: The Demonstration Experiment in: Journal of Applied Meteorology and Climatology Volume 42 Issue 7 (2003)*. Results of On-Top Glaciogenic Cloud Seeding in Thailand. Part I: The Demonstration Experiment. https://journals.ametsoc.org/view/journals/apme/42/7/1520-0450_2003_042_0920_roogcs_2.0.co_2.xml?tab_body=pdf

60. Xie, Y., Zhou, M., Hunt, K.M.R. et al. Recent PM2.5 air quality improvements in India benefited from meteorological variation. Nat Sustain 7, 983–993 (2024). https://doi.org/10.1038/s41893-024-01366-y
61. Xie, Y., Zhou, M., Hunt, K.M.R. et al. Recent PM2.5 air quality improvements in India benefited from meteorological variation. Nat Sustain 7, 983–993 (2024). https://doi.org/10.1038/s41893-024-01366-y
62. Yadav, R.K., Rupa Kumar, K. & Rajeevan, M. Characteristic Features of Winter Precipitation and Its Variability Over Northwest India. *J Earth Syst Sci* **121**, 611–623 (2012). https://doi.org/10.1007/s12040-012-0184-8
63. Zhao, X., Sun, Y., Zhao, C., & Jiang, H. (2020). Impact of precipitation with different intensity on PM2. 5 over typical regions of China. *Atmosphere*, *11*(9), 906, https://doi.org/10.3390/atmos11090906